

1

Higgs

1.1

Introduction

The Standard Model (SM) is a theory to explain interactions of elementary particles at the most fundamental level. Its essence can be summarized as follows.

- 1) The fundamental constituent blocks of matter are quarks and leptons.
- 2) The mathematical framework for the force dynamics are gauge theories.
- 3) The vacuum is in a kind of super-conducting phase.

The phase transition to the pseudo-superconducting phase is the action of the Higgs field. However, the precise dynamics of the symmetry breaking is not known. For this reason, the SM was believed to lose its predictive power on phenomena at energy scale over $O(\text{TeV})$.

The electroweak (EW) interaction of fermions (i.e., quarks and leptons) is mediated by the gauge particles W^\pm , Z^0 . The role of the Higgs is to attach masses to the gauge particles and fermions without breaking the gauge symmetry. The symmetry is broken spontaneously by self-interactions of the Higgs field, which is referred to as the *Higgs mechanism*. It is the fundamental framework of the SM, and its basic notion is well founded because the SM reproduces experiments quite well.

However, it is also the least known sector in the SM. The Higgs potential was chosen for its simplicity and may not be realized in the real world. In fact, evidences are accumulating that some kind of symmetry is at work in the Higgs sector that is not yet identified. Only direct production of the Higgs particle and detailed investigation of its dynamical properties will clarify the properties of the Higgs field.

The gauge sector of the SM has been proved to reproduce experiments to a high degree of precision. From its perspective, the Higgs sector's role is only to provide masses to otherwise massless particles, and nothing else matters. Very little information on the Higgs is obtained from the gauge sector. Besides, there is no guiding principle to unify the mass generation mechanism of the fundamental

fermions (aka the Yukawa interaction), and this remains the weak point of the SM to qualify it as a unified theory. If a defect exists in the so-far-infallible SM, it is highly probable that it is found in the Higgs sector. As the Higgs particle was discovered at the large hadron collider (LHC) in 2012,¹⁾ the next urgent problem of the SM is to elucidate its dynamical structure.

In this chapter, we will discuss the fundamental properties of the Higgs particle and theoretical constraints on its mass, as well as how to proceed after its discovery [3–5]. We review methods to discover the Higgs, because properties of the Higgs are best elucidated by its detection strategy. We will also discuss the likely possibilities of the Higgs properties that go beyond the SM, including the supersymmetric extension and the possibility of strong dynamical breaking of the EW symmetry.

1.2 Higgs Interactions

1.2.1

Standard Model

The symmetry of the EW interaction in the SM is based on a mixture of $SU(2)$ and $U(1)$. The weak force in its original form, that is, before mixing and spontaneous symmetry breakdown, has chiral symmetry.

In $SU(2)$ terminology, the weak force carriers constitute an isospin triplet. All the left-handed fermions constitute doublets. All the right-handed particles belong to $SU(2)$ singlets ($I = I_3 = 0$), that is, they do not carry weak charges. In the SM, all the leptons can be classified by their isospin component as

$$\text{Leptons} \quad \begin{cases} I_3 = +\frac{1}{2} \\ I_3 = -\frac{1}{2} \\ I = I_3 = 0 \end{cases} \quad \Psi_L = \begin{pmatrix} \nu_e \\ e^- \end{pmatrix}_L, \quad \begin{pmatrix} \nu_\mu \\ \mu^- \end{pmatrix}_L, \quad \begin{pmatrix} \nu_\tau \\ \tau^- \end{pmatrix}_L \quad (1.1)$$

$$e_R^-, \mu_R^-, \tau_R^-$$

The leptons that have $I_3 = 1/2$, that is, the neutrinos, are electrically neutral and those that have $I_3 = -\frac{1}{2}$ have electric charge $Q = -1$ in units of the positron charge.

1) The LHC is located at CERN in Geneva, and is designed to reach the total center-of-mass energy $\sqrt{s} = 14$ TeV with luminosity $5 \times 10^{34} \text{ cm}^{-2} \text{ S}^{-1}$. The detectors comprise two general-purpose detectors (A Toroidal

LHC Apparatus, ATLAS, and compact muon solenoid, CMS) and two dedicated detectors, LHCb for B-physics and ALICE for heavy-ion physics.

In the SM, right-handed neutrinos do not exist.²⁾ For the quarks

$$\text{Quarks} \quad \begin{cases} I_3 = +\frac{1}{2} & \begin{pmatrix} u \\ d' \end{pmatrix}_L \\ I_3 = -\frac{1}{2} & \begin{pmatrix} c \\ s' \end{pmatrix}_L \\ I = I_3 = 0 & u_R, d_R, c_R, s_R, t_R, b_R \end{cases} \quad (1.2)$$

where $D'^T \equiv (d', s', b')^T$ are the Cabibbo–Kobayashi–Maskawa (CKM) rotated fields:

$$\begin{bmatrix} d' \\ s' \\ b' \end{bmatrix} = V_{\text{CKM}} \begin{bmatrix} d \\ s \\ b \end{bmatrix}, \quad V_{\text{CKM}} = \begin{bmatrix} V_{ud} & V_{us} & V_{ub} \\ V_{cd} & V_{cs} & V_{cb} \\ V_{td} & V_{ts} & V_{tb} \end{bmatrix} \quad (1.3)$$

The quarks with $I_3 = 1/2$ have $Q = 2/3$, and those with $I_3 = -1/2$ have $Q = -1/3$. Each quark carries another degree of freedom, that is, three colors, which are the source of the strong interaction. Its dynamics constitutes a field of its own, but in the discussion of the EW force, we put aside their interactions and simply consider the fact that they only provide three extra degrees of freedom.

We denote the Higgs doublet³⁾ the left-handed electron doublet, and the gauge boson triplet as

$$\Phi = \begin{bmatrix} \phi^+ \\ \phi^0 \end{bmatrix}, \quad \Psi_L = \begin{bmatrix} \nu_L \\ e_L^- \end{bmatrix}, \quad \mathbf{W}_\mu = (W_\mu^+, W_\mu^0, W_\mu^-) \quad (1.4)$$

The original Lagrangian of the EW interaction before mixing and spontaneous symmetry breaking is given by

$$\begin{aligned} \mathcal{L}_{\text{EW}} = & \bar{\Psi}_i \gamma^\mu D_\mu \Psi - \frac{1}{4} \mathbf{F}_{\mu\nu} \cdot \mathbf{F}^{\mu\nu} - \frac{1}{4} B_{\mu\nu} B^{\mu\nu} \\ & + (D_\mu \Phi)^\dagger (D^\mu \Phi) - V(\Phi) - \gamma_e [\bar{e}_R (\Phi^\dagger \Psi_L) + (\bar{\Psi}_L \Phi) e_R] \end{aligned} \quad (1.5)$$

$$\mathbf{F}_{\mu\nu} = \partial_\mu \mathbf{W}_\nu - \partial_\nu \mathbf{W}_\mu - g_W \mathbf{W}_\mu \times \mathbf{W}_\nu \quad (1.6a)$$

$$B_{\mu\nu} = \partial_\mu B_\nu - \partial_\nu B_\mu \quad (1.6b)$$

2) In reality, they do exist as demonstrated by the discovery of the neutrino oscillation. In the context of this textbook, no inconvenience is encountered by assuming the massless neutrino in this chapter and it greatly simplifies discussions. The neutrino oscillation phenomena will be treated in the next chapter.

3) We loosely call Φ or all the four scalar fields as the Higgs. But to be more accurate, after the symmetry breakdown, ϕ^+ and the imaginary part of ϕ^0 are absorbed by the gauge bosons to give them mass, and only one field, the real part of ϕ^0 , remains as a massive physical field. It is renamed as h , which is the genuine Higgs field.

$$D_\mu = \partial_\mu + ig_W \mathbf{W}_\mu \cdot \mathbf{t} + i(g_B/2)Y \quad (1.6c)$$

$$V(\Phi) = \lambda \left(|\Phi|^2 + \frac{\mu^2}{2\lambda} \right)^2 \quad \lambda > 0 \quad (1.6d)$$

where \mathbf{t} is the generator of the $SU(2)$ symmetry group. Notice that, except in the Higgs potential, there are no mass terms (quadratic term in the fields) in the Lagrangian.⁴⁾

We shall use ν_e, e^- , and so on, to denote the quantized fields, that is, $\nu_e(x) = \psi_{\nu_e}(x)$, $e^-(x) = \psi_e(x)$, and so on, where there is no confusion. Here, we have written down only the Lagrangian of $\Psi^T = (\nu_e, e^-)$, which will be needed in the following discussions. The Lagrangian for other fermions can be written down similarly.

The first line of Eq. (1.5) is referred to as the *gauge sector* and the second line as the *Higgs sector*. $V(\Phi)$ is the self-interacting potential of the Higgs field. The whole expression satisfies the $SU(2) \times U(1)$ gauge symmetry manifestly. It is important to remember that both the gauge and the Higgs sectors are constructed to respect the gauge symmetry separately. The last term of Eq. (1.5), referred to as the *Yukawa interaction*, was added to generate fermion masses. It can be written down as

$$\bar{e}_R(\Phi^\dagger \Psi_L) + (\bar{\Psi}_L \Phi) e_R = \bar{e}_R \nu_{eL} \phi^- + \bar{\nu}_{eL} e_R \phi^+ + \bar{e}_R e_L \phi^{0\dagger} + \bar{e}_L e_R \phi^0 \quad (1.7)$$

The self-interaction of the Higgs is the cause of the spontaneous symmetry breakdown of the $SU(2)_L \times U(1)$, giving mass to the gauge bosons and the fermions.

Electroweak mixing: As the neutral component of \mathbf{W} and B couple to the same fermions, mixing occurs, and physical neutral gauge bosons γ and Z^0 are expressed as

$$\begin{aligned} Z_\mu &= \frac{1}{\sqrt{g_W^2 + g_B^2}} (g_W W_\mu^0 - g_B B_\mu) \equiv \cos \theta_W W_\mu^0 - \sin \theta_W B_\mu \\ \gamma_\mu &= \frac{1}{\sqrt{g_W^2 + g_B^2}} (g_B W_\mu^0 + g_W B_\mu) \equiv \sin \theta_W W_\mu^0 + \cos \theta_W B_\mu \end{aligned} \quad (1.8)$$

where θ_W (or $\sin \theta_W$) is referred to as the *Weinberg angle*. As a result, the gauge interaction of the fermions is described by the interaction Lagrangian

$$\begin{aligned} -\mathcal{L}_{\text{int}} &= \frac{g_W}{2} \bar{\Psi}_L \gamma^\mu \mathbf{W}_\mu \cdot \boldsymbol{\tau} \Psi_L + \frac{g_B}{2} \bar{\Psi} \gamma^\mu B_\mu \Psi \\ &= \frac{g_W}{\sqrt{2}} \bar{\Psi}_L \gamma^\mu \left(W_\mu^+ \tau_+ + W_\mu^- \tau_- \right) \Psi_L \\ &\quad + g_Z \bar{\Psi} \gamma^\mu (I_{3L} - Q \sin^2 \theta_W) \Psi Z_\mu + e \bar{\Psi} \gamma^\mu Q \Psi A_\mu \end{aligned} \quad (1.9)$$

4) The quadratic as well as the quartic terms exist in the SM Higgs potential. But in some extensions of the SM, they are absent in the tree

Lagrangian. They are generated radiatively as a result of the Higgs–gauge interaction [6].

where $\tau_{\pm} = (\tau_1 \pm \tau_2)/2$ and the coupling strength of Z and A is given by

$$g_Z = \frac{g_W}{\cos \theta_W} = \frac{e}{\sin \theta_W \cos \theta_W}, \quad e = g_W \sin \theta_W \quad (1.10)$$

1.2.2

Lagrangian After Symmetry Breaking

The whole Lagrangian of the SM satisfies manifestly the $SU(2) \times U(1)$ gauge symmetry. Symmetry breaking occurs when the coefficient of the quadratic term in the potential is driven negative. It happens when the environmental temperature goes below a certain critical temperature. The potential minimum moves away from $\Phi = 0$, that is, the vacuum moves to where one of its components is finite.⁵⁾

We say that the Higgs field has acquired the vacuum expectation value (VEV) $\langle \phi^0 \rangle = v/\sqrt{2}$. The factor $1/\sqrt{2}$ is conventional. The vacuum is no longer at $\Phi = 0$. As the symmetry around two different points are different, that is, the potential has no original symmetry at the new vacuum point, we say the symmetry is broken. In the terminology of condensed matter physics, the ground state is now Bose condensate, with v representing an order parameter. Physical phenomena that are observed as excitations from the new vacuum no longer exhibit the original symmetry. Notice, however, that the symmetry of the potential is not really lost. Physical phenomena are generally small excitations around the vacuum, which is a local minimum of the potential. Power expansions of the potential around $\Phi = 0$ and around $\phi^0 = v/\sqrt{2}$ have different mathematical expression. Naturally, a physical phenomenon interpreted from viewpoint of the new vacuum look different from that in the old vacuum. Mathematically, it is possible to work using the field variables based on the old vacuum compromising easy physical interpretation. In this sense, the symmetry is not broken but hidden.

The condition that $\phi^0 = v/\sqrt{2}$ is at potential minimum sets the value of μ^2 .

$$\left. \frac{\partial V}{\partial \phi^0} \right|_{\phi^0=v/\sqrt{2}} = 0 \quad \xrightarrow{\text{SB}} \quad \mu^2 = -\lambda v^2 \quad (1.11)$$

where SB denotes the symmetry breaking. Without loss of generality, the Higgs field before and after the symmetry breakdown can be reexpressed as follows:

$$\Phi = e^{i\frac{\omega}{v} \cdot \frac{z}{2}} \begin{bmatrix} 0 \\ \phi^0 \end{bmatrix} \equiv U^{-1} \begin{bmatrix} 0 \\ \phi^0 \end{bmatrix} \quad \xrightarrow{\text{SB}} \quad \Phi' = U\Phi = \begin{bmatrix} 0 \\ \frac{v+h}{\sqrt{2}} \end{bmatrix} \quad (1.12)$$

“ h ” is the physical Higgs field we are interested in and is most significant in this chapter. The Higgs components ω in the phase are removed by the gauge transformation U and become the third component of the massive gauge bosons. In mathematical language, the ω fields are gauged away. Stated differently, the spontaneous symmetry breakdown is equivalent to choosing a gauge and fixing it. We write the covariant derivative and the Higgs doublet after the symmetry

5) It is customary to choose the vacuum point at $\phi^0 = \frac{v}{\sqrt{2}}$, $\text{Im}[\phi^0] = \phi^+ = \phi^- = 0$.

breaking as

$$D_\mu \Phi \xrightarrow{SB} UD_\mu U^{-1}U\Phi \equiv D'_\mu \Phi' = \left[\partial_\mu + ig_W \mathbf{W}'_\mu \cdot \mathbf{t} + i\frac{g_B}{2} B_\mu \right] \begin{bmatrix} 0 \\ \frac{\nu+h}{\sqrt{2}} \end{bmatrix} \quad (1.13)$$

Then we rename $D'_\mu \Phi'$, \mathbf{W}'_μ as $D_\mu \Phi$, \mathbf{W}_μ .

In terms of the newly defined field variables, the Higgs sector of the Standard Model Lagrangian is reexpressed as

$$\begin{aligned} \mathcal{L}_h &= (D_\mu \Phi)^\dagger (D_\mu \Phi) - \lambda \left(\Phi^\dagger \Phi - \frac{v^2}{2} \right)^2 - \gamma_e [\bar{e}_R (\Phi^\dagger \Psi_L) + (\bar{\Psi}_L \Phi) e_R] \\ &\xrightarrow{SB} \frac{1}{2} (\partial_\mu h \partial^\mu h - m_h^2 h^2) - \left(\lambda v h^3 + \frac{\lambda}{4} h^4 \right) \\ &\quad + 2(\sqrt{2}G_F)^{\frac{1}{2}} h \left(m_W^2 W_\mu^+ W^{-\mu} + \frac{m_Z^2}{2} Z_\mu Z^\mu \right) \\ &\quad + \sqrt{2}G_F h^2 \left(m_W^2 W_\mu^+ W^{-\mu} + \frac{m_Z^2}{2} Z_\mu Z^\mu \right) \\ &\quad + \sum_f \left(m_f + \sqrt{2}G_F m_f h \right) \bar{f} f \end{aligned} \quad (1.14)$$

where the electron (e) term has been expanded to include all the fermions (f). The coupling constants G_F , γ_f , and λ are related to the masses by

$$g_W = \frac{e}{\sin \theta_W} = 2(\sqrt{2}G_F)^{\frac{1}{2}} m_W \quad (1.15a)$$

$$g_Z = \frac{e}{\sin \theta_W \cos \theta_W} = 2(\sqrt{2}G_F)^{\frac{1}{2}} m_Z \quad (1.15b)$$

$$\frac{1}{v} = \frac{g_W}{2m_W} = (\sqrt{2}G_F)^{\frac{1}{2}} = \frac{1}{246 \text{ GeV}} \quad (1.15c)$$

$$m_h^2 = 2\lambda v^2, \quad m_f = \frac{\gamma_f v}{\sqrt{2}} \quad (1.15d)$$

Notice that the mass of the fermions is directly proportional to the Yukawa coupling constant. After the symmetry breaking, the SM has mass terms for the gauge bosons, fermions, and the Higgs itself. As one can see from the above expressions, the coupling strength of the Higgs is directly proportional to the mass of the particles to which it couples. The self-coupling strength λ is also proportional to the mass of the Higgs (squared). λ is an unknown parameter, hence the Higgs mass cannot be determined a priori. The Lagrangian Eq. (1.14) is the starting point of the Higgs interactions. Feynman rules for the Higgs interaction are given in Figure 1.1.

1.2.3

Decay Modes

Decays to a Fermion Pair Once the Lagrangian is given, it is straightforward to write down the matrix element for the decay of the Higgs to two fermions in the

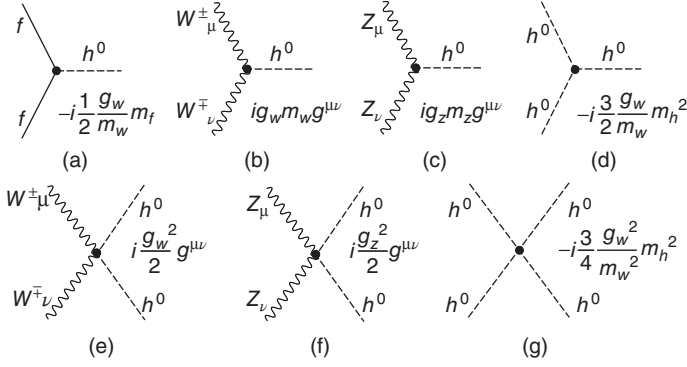


Figure 1.1 Feynman rules for the Higgs interaction. The coupling constants γ_f , λ , and so on, are reexpressed in terms of the mass of the particles to which the Higgs couples.

tree approximation.

$$\mathcal{M}(h \rightarrow f\bar{f}) = (\sqrt{2}G_F)^{\frac{1}{2}} m_f \bar{u}(p_1)v(p_2) \quad (1.16)$$

The decay width becomes

$$\Gamma(h \rightarrow f\bar{f}) = \frac{N_c G_F m_f^2 m_h}{4\sqrt{2}\pi} \left(1 - \frac{4m_f^2}{m_h^2}\right)^{3/2} \quad (1.17)$$

where $N_c = 1$ for leptons and $N_c = 3$ for quarks. As the coupling strength is proportional to the mass, the dominant mode is the decay to the heaviest fermions that is allowed energetically. For $m_h < 2m_W$, $h \rightarrow b\bar{b}$ is the most dominant decay mode.

Decay to Bosons If the Higgs mass is greater than $2m_W$ or $2m_Z$, it can decay to W or Z pairs. The decay amplitude to the W pair can be calculated from the third line of Eq. (1.14) to give

$$\mathcal{M}(h \rightarrow W^+ W^-) = 2(\sqrt{2}G_F)^{\frac{1}{2}} m_W^2 \varepsilon_\mu^*(p_1, \lambda_1) \varepsilon^\mu(p_2, \lambda_2) \quad (1.18)$$

where $p_1, p_2, \lambda_i, \varepsilon^\mu$ denote the momenta, polarization state, and polarization vectors of W^\pm . Then the decay width to pairs with transverse ($\lambda = \pm$) and longitudinal

($\lambda = 3$) polarization are given by

$$\Gamma(h \rightarrow W_T W_T) = \frac{G_F m_W^4}{2\sqrt{2}\pi m_h} (1 - 4\gamma_W^2)^{1/2} \quad (1.19a)$$

$$\Gamma(h \rightarrow W_L W_L) = \frac{G_F m_h^3}{8\sqrt{2}\pi} (1 - 2\gamma_W^2)^2 (1 - 4\gamma_W^2)^{1/2} \quad (1.19b)$$

$$\Gamma(h \rightarrow W^+ W^-) = 2\Gamma(h \rightarrow W_T W_T) + \Gamma(h \rightarrow W_L W_L) \quad (1.19c)$$

$$= \frac{G_F m_h^3}{8\sqrt{2}\pi} (1 - 4\gamma_W^2 + 12\gamma_W^4)(1 - 4\gamma_W^2)^{1/2} \quad (1.19d)$$

$$\text{where } \gamma_W = \frac{m_W}{m_h}, \quad \gamma_Z = \frac{m_Z}{m_h} \quad (1.19e)$$

From the above expression, one sees that, if $m_h \gg m_W$, the W pairs that decayed from the Higgs are dominantly polarized longitudinally. The decay width to Z can be obtained similarly.

$$\Gamma(h \rightarrow ZZ) = \frac{G_F m_h^3}{16\sqrt{2}\pi} (1 - 4\gamma_Z^2 + 12\gamma_Z^4)(1 - 4\gamma_Z^2)^{1/2} \quad (1.20)$$

There is a factor 2 difference between the W pair decay modes which originate from the Bose statistics for identical particles. For $m_h \gg m_Z$, $\Gamma(h \rightarrow WW) \approx 2\Gamma(h \rightarrow ZZ)$.

Carrying out calculations for all possible decay modes and adding all, one can obtain the total decay width of the Higgs particle. If $m_h < 2m_W$, the main decay mode is $h \rightarrow b\bar{b}$. If $m_h > 2m_W$, it mainly decays to WW and ZZ . Figure 1.2 shows the total decay width and branching ratios of the Higgs as a function of the Higgs mass.

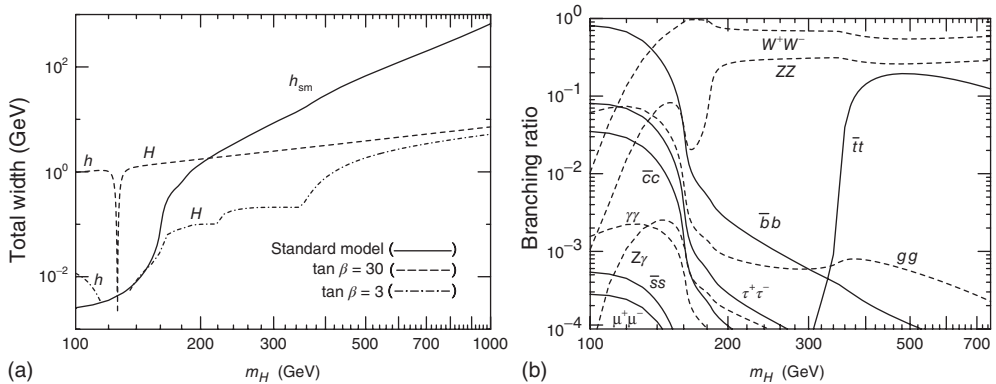


Figure 1.2 (a) Total decay width of the Standard Model Higgs. Also shown are those of two neutral Higgs (h and H) for the supersymmetric extension of the Higgs sector. $\tan \beta = \nu_2/\nu_1$ is the ratio of the

two vacuum expectation values of the condensed Higgs field of the supersymmetry. (b) Branching ratios of the dominant decay modes of the Standard Model Higgs boson. (Reproduced with permission of [7].)

The reason why $\Gamma(h \rightarrow ZZ)$ decreases around $m_h \sim 160$ GeV is because the channel $h \rightarrow WW$ opens here.

1.3 Mass

The Higgs was discovered in 2012 with mass $m_h \simeq 125$ GeV. However, its mass value is not just one parameter among many. The size of the Higgs mass has an important significance in considering the mechanism of the spontaneous symmetry breakdown and the future scenario of the physics beyond the SM.

1.3.1

Predictions from EW Data

Much information had been obtained from radiative correction data at the large electron–positron (LEP) collider and the Tevatron. As we learned in Chapter 5 of [2], main contributions to the radiative corrections come from heavy particles, namely top and the Higgs. From the Z decay and W production data, one can determine the value of the Weinberg angle $\sin \theta_W$ and the coupling ratio ρ of the neutral versus charged current interaction.

$$\begin{aligned} \rho &\equiv \rho_0(1 + \Delta\rho) \equiv \frac{G_N}{G_W} \text{ } ^6) = \frac{m_W^2}{m_Z^2 \cos^2 \theta_W^2} \\ \Delta\rho &= \delta\rho_t + \delta\rho_h + \dots \\ \delta\rho_t &\simeq \frac{3G_F m_t^2}{8\sqrt{2}\pi^2} \approx 0.0096 \left(\frac{m_t}{173 \text{ GeV}} \right)^2 \\ \delta\rho_h &\simeq -\frac{3G_F m_Z^2 \sin^2 \theta_W}{8\sqrt{2}\pi^2} \left(\ln \frac{m_h^2}{m_W^2} - \frac{5}{6} \right)^2 \end{aligned} \quad (1.21)$$

As the top mass was determined by direct productions at the Tevatron, its value can be used to test the validity of the EW prediction. The observed top mass agreed quite well with the prediction given by the precision EW data [8]. It is a major triumph of the SM. Now that the top mass is given, Eq. (1.21) can be used to predict the Higgs mass. As the Higgs contribution is logarithmic, sensitivity to the Higgs mass is weak. An overall fit to the world data for the mass value prior to LHC operation is given in Figure 1.3.

In this way, one can predict the value of the SM Higgs boson mass. A very recent analysis shows [10, 12]

$$m_h = 120_{-05}^{+12} \text{ GeV} \quad (1.22)$$

6) G_N is the four-Fermi coupling constant of the neutral current interaction corresponding to G_F of the charged current. At the tree level, $G_N = G_F$. Note that G_N is also used to denote the Newton's gravitational constant elsewhere.

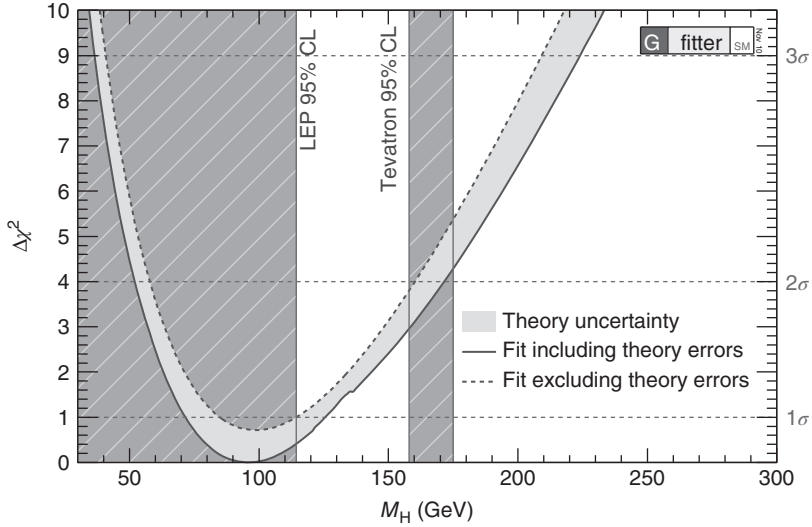


Figure 1.3 Higgs mass exclusion plot as a function of the Higgs mass before the Higgs discovery. (Reproduced with permission of [9–12].)

leading to a 95% CL limit in the SM

$$114 < m_h < 144 \text{ GeV} \tag{1.23}$$

Here we discuss the theoretical implications of this value.

1.3.2

Vacuum stability

Comparison of theoretical radiative corrections with precision experimental data predicts a rather low Higgs mass. Let us consider first what theoretical constraints can be obtained from the SM framework. A constraint for the lower mass limit can be obtained from vacuum stability. One condition for spontaneous symmetry breaking of the vacuum was that λ , that is, the coefficient of the quartic term in the Higgs potential, must remain positive.

$$V(\phi) = \lambda \left(\Phi^\dagger \Phi - \frac{v^2}{2} \right)^2 = V(0) - \frac{m_h^2}{2} \Phi^\dagger \Phi + \lambda (\Phi^\dagger \Phi)^2 \tag{1.24}$$

$$m_h^2 = 2\lambda v^2$$

A negative value of λ makes the vacuum unstable for large values of $|\Phi|$. Positivity of λ is guaranteed only at the tree level. Taking into account the radiative corrections to the Higgs propagator, the value of the coupling constant λ is governed at one-loop

level by the following renormalization group equation [3, 13].⁷⁾

$$\frac{d\lambda}{d\tau} = \beta(\lambda) = \frac{3}{4\pi^2}(\lambda - \lambda_+)(\lambda - \lambda_-), \quad \lambda_- \leq \lambda_+ \quad (1.25a)$$

$$\beta(\lambda) = \frac{1}{16\pi^2} \left[12\lambda^2 + 6\lambda\gamma_t^2 - 3\gamma_t^4 - \frac{3}{2}\lambda(g_W^2 + g_B^2) + \frac{3}{16} \{2g_W^4 + (g_W^2 + g_B^2)^2\} \right] \quad (1.25b)$$

where $\tau = \ln(Q^2/Q_0^2)$, $\gamma_t = \sqrt{2}m_t/\nu$ is the Yukawa coupling constant, and g_W and g_B are the $SU(2)$ and $U(1)$ gauge coupling constants, respectively. Contributions from quarks other than the top are neglected because the coupling strength is directly proportional to its mass value. The λ that obeys Eq. (1.25) is no longer a constant, but a dynamical variable that depends on τ . The original λ can be considered as that defined by the condition $\lambda = \lambda(Q)|_{Q=Q_0(=\nu)}$. Inclusion of the radiative corrections changes the potential shape, and hence the VEV of the Higgs ϕ^0 has to be redefined as that which gives the minimum to the modified potential.

Let us disregard, for simplicity, the Q^2 dependence of γ_t, g_W, g_B . Then, $\beta(\lambda)$ is a quadratic function of λ and has zeros at $\lambda = \lambda_{\pm}$. For $4m_t^4 > 2m_W^4 + m_Z^4$, we have $\lambda_- < 0 < \lambda_+$. The solution depends on the magnitude of the initial value $\lambda_0 = \lambda(Q_0)$. Depending on whether $\lambda_0 > \lambda_+$ or $0 < \lambda_0 < \lambda_+$, the solution to Eq. (1.25) is given by

$$\frac{\lambda - \lambda_-}{\lambda - \lambda_+} = \pm A e^{-\delta\tau} \quad (1.26a)$$

$$\delta = \frac{3}{4\pi^2}(\lambda_+ - \lambda_-) \quad (1.26b)$$

For $\lambda_0 > \lambda_+$, the value of λ will always remain positive. If $0 < \lambda_0 < \lambda_+$, the beta function is negative ($\beta(\lambda) < 0$). In this case, for sufficiently large Q , λ becomes negative at a certain value $Q = \Lambda$. The resultant potential is negative at large ϕ and has no minimum. In other words, the vacuum is unstable. This happens for small λ , in which case the top quark contribution dominates and drives λ to a negative value for sufficiently large Q^2 . For small λ , Eq. (1.25) becomes

$$\frac{d\lambda}{d\tau} \simeq \frac{1}{16\pi^2} \left[-3\gamma_t^4 + \frac{3}{16} \{2g_W^4 + (g_W^2 + g_B^2)^2\} \right] \quad (1.27)$$

To provide an intuitive understanding through easy analytic implementation, we assume γ_t, g_W , and g_B are constant, and integrate Eq. (1.27) and obtain

$$\lambda(\Lambda) = \lambda(\nu) + \frac{1}{16\pi^2} \left[-3\gamma_t^4 + \frac{3}{16} \{2g_W^4 + (g_W^2 + g_B^2)^2\} \right] \ln \left(\frac{\Lambda^2}{\nu^2} \right) \quad (1.28)$$

To ensure that $\lambda(\Lambda)$ remains positive, the Higgs mass ($= 2\lambda\nu^2$) must satisfy

$$m_h^2 > \frac{\nu^2}{8\pi^2} \left[3\gamma_t^4 - \frac{3}{16} \{2g_W^4 + (g_W^2 + g_B^2)^2\} \right] \ln \left(\frac{\Lambda^2}{\nu^2} \right) \quad (1.29)$$

More elaborate calculation can be carried out by integrating Eq. (1.25). A detailed calculation incorporating two loop-level radiative corrections has been carried out in [14] and gives the lower limit as a function of Λ , which is shown as the lower curve of Figure 1.4.

7) For basics of the renormalization group equation, see Section 7.2 of [2].

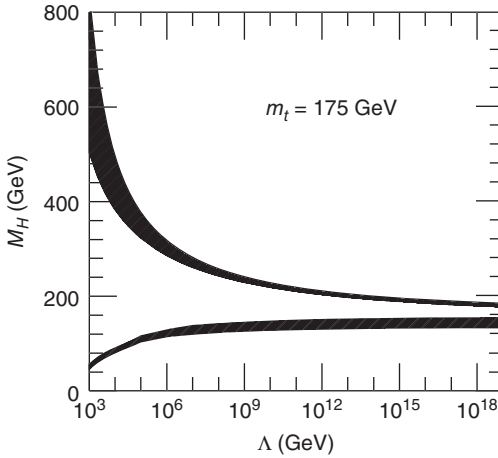


Figure 1.4 Triviality (upper) bound and vacuum stability (lower) bound on the Higgs boson mass as functions of the new physics or cutoff scale Λ for a top quark mass $m_t = 175 \pm 6$ GeV and $\alpha_s(m_Z) = 0.118 \pm 0.002$. The allowed region lies between the bands, and the colored/shaded bands illustrate the impact of various uncertainties. (Reproduced with permission of [13–15].)

A state-of-the-art quantum correction at the next-to-next-to-leading order (NNLO) calculations has been carried out recently [16]. Assuming the validity of Eq. (1.25) all the way up to the grand unified theory (GUT) energy, one obtains

$$m_h > 129.4 + 1.4 \times \left(\frac{m_t(\text{GeV}) - 173.1}{0.7} \right) - 0.5 \times \left(\frac{\alpha_s(m_Z) - 0.1184}{0.0007} \right) \pm 1.0 \text{ GeV} \quad (1.30)$$

1.3.3

Theoretical Upper Limit

Perturbative Unitarity The Higgs mass cannot be indefinitely large. The simplest argument is supplied by the unitarity condition of the tree-level scattering amplitude. Let us consider scattering of the gauge boson W . Feynman diagrams that contribute to the elastic scattering are presented in Figure 1.5.

The gauge invariance provides a compensating mechanism for particular amplitudes from diverging to infinity and suppresses divergence to at most the logarithmic level (see arguments in Chapter I of [2]). For instance, each amplitude in Figure 1.5a–c grows $\sim s^2$ but combined together they cancel each other and the divergence is at most $\sim s$. Terms that grow by $\sim s$ are cancelled by the Higgs intermediate processes (Figure 1.5d,e), and the resultant overall divergence is at most $\sim \ln s$. At the tree level, the contribution of the Higgs intermediate scattering amplitude is approximately given by [17]

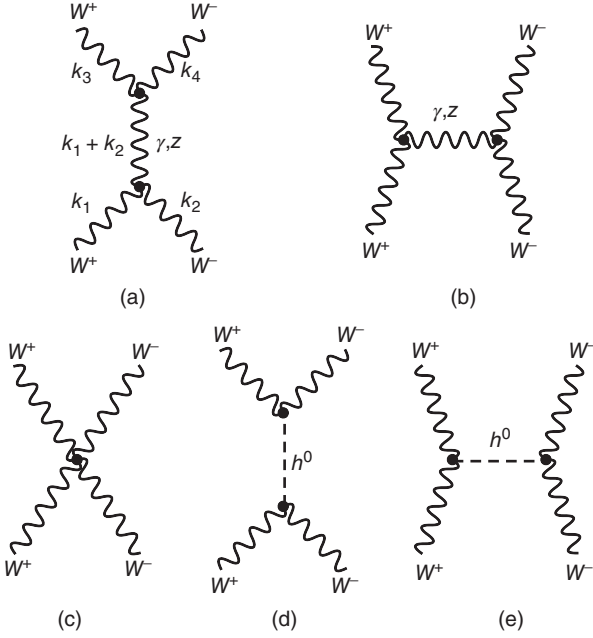


Figure 1.5 Feynman diagrams for $W^+ W^- \rightarrow W^+ W^-$.

$$\mathcal{M}(W_L^+ W_L^- \rightarrow W_L^+ W_L^-) = -\sqrt{2} G_F m_h^2 \left[\frac{s}{s - m_h^2} + \frac{t}{t - m_h^2} \right] + O\left(\frac{m_W^2}{s}\right) \quad (1.31)$$

We have considered only the scattering amplitude by longitudinally polarized W s because they are the ones that give bad divergence at large s . This is due to the fact that the longitudinal polarization produces a factor $\sim p_\mu p_\nu / m_W^2$ in the denominator of the gauge boson propagator. Decomposing the scattering amplitude into partial waves, it can be expressed as

$$\mathcal{M} = 16\pi \sum (2J + 1) a_J(s) P_J(\cos \theta) \quad (1.32)$$

At high energy ($s \gg m_W^2$), the S wave amplitude can be extracted to give

$$a_0(W_L W_L \rightarrow W_L W_L) = -\frac{G_F m_h^2}{8\sqrt{2}\pi} \left[2 + \frac{m_h^2}{s - m_h^2} - \frac{m_h^2}{s} \ln \left(1 + \frac{s}{m_h^2} \right) \right] \quad (1.33)$$

At sufficiently high energy, the first term is dominant. The unitarity requires $|a_0| \leq 1$. As the Born amplitude is real, the requirement becomes $|\text{Re}A_0| \leq 1/2$. Then

$$m_h \leq \left[\frac{2\sqrt{2}\pi}{G_F} \right]^{\frac{1}{2}} = 872 \text{ GeV} \quad (1.34)$$

Another argument one may use is that, for the Higgs to qualify as an elementary particle, its mass has to exceed its width, that is, $m_h > \Gamma_h$. This gives the condition

$$\Gamma(h \rightarrow WW + ZZ) \simeq \frac{3G_F m_h^3}{16\sqrt{2}\pi} < m_h \quad (1.35)$$

and $m_h < 1.4$ TeV is obtained. However, if the Higgs mass is as large as this, it means λ is also very large ($\lambda/4\pi \geq O(1)$) because $m_h^2 = 2\lambda v^2$. The self-interaction of the Higgs is strong, and one questions the validity of the perturbative calculation. All one can claim is that the Higgs mass should be less than ~ 1 TeV.

Triviality Another constraint on the upper limit can be obtained from the renormalization group equation. As we are discussing a possible outcome at large λ , we can neglect all the terms except λ in Eq. (1.25). Then we can obtain the following solution. Setting $Q_0 = v$

$$\frac{1}{\lambda(v)} - \frac{1}{\lambda(Q)} = \frac{3}{4\pi^2} \ln\left(\frac{Q^2}{v^2}\right) \quad (1.36)$$

In order for the above equation to be valid in the perturbative approach, $\lambda(Q)$ has to be finite and reasonably small. Then, $\lambda(v)$ can only vanish in the limit $Q \rightarrow \infty$. This means that the equation of motion that the Higgs obeys must be a free equation without interaction. It is a “trivial” solution. Rewriting the above formula, one obtains

$$\lambda(Q) = \frac{\lambda(v)}{1 - \frac{3}{4\pi^2} \lambda(v) \ln\left(\frac{Q^2}{v^2}\right)} \quad (1.37)$$

For sufficiently large Q^2 , the denominator vanishes, which is referred to as the *Landau pole*, and the value of λ diverges. As the perturbative treatment fails for large λ , it means that the equation that the Higgs field satisfies has to be considered as an effective theory valid only at low energy. The perturbative approach may be justified for $Q \lesssim \Lambda$, for which $\lambda(Q)$ remains finite and sufficiently small. The maximum value of $\lambda(v)$ within the constraint can be obtained from Eq. (1.36) by setting $\lambda(Q) = \infty$. Therefore

$$m_h^2 \leq 2v^2 \max[\lambda(v)] = \frac{8\pi^2 v^2}{3 \ln(\Lambda^2/v^2)} \quad (1.38)$$

If we assume that the perturbative approach is valid and λ remains small until $\Lambda = M_{\text{Planck}} \simeq 10^{19}$ GeV, we obtain $m_h < 150$ GeV. This value does not depend on how we set the value of $\lambda(Q)$. If we use $\lambda(Q) = 1$ instead of $\lambda(Q) = \infty$, the numerical value of the Higgs mass is almost the same.

This is an interesting fact. Suppose there is a grand unification at large Q ($\sim 10^{16}$ GeV), and no new physics comes in until the grand unification scale, the Higgs has to be light. The supersymmetry (SUSY) approach we discuss later, in which the Higgs is considered as elementary, falls in this category. Conversely, if the Higgs is heavy, for which it could be a composite, the new physics will appear at relatively low energy. Assuming it happens actually, we may rephrase the existence

condition of the Higgs as $m_h < \Lambda$, which leads to $m_h \lesssim 800$ GeV. The upper curve of Figure 1.4 shows how the upper limit of the Higgs mass changes as a function of the cutoff Λ . The allowed range of the Higgs mass depends on where we set the cutoff Λ . If we assume no new physics until the GUT energy ($\sim 10^{16}$ GeV), we have a severe constraint $140 \lesssim m_h \lesssim 200$ GeV. The mass of the discovered Higgs is less than the lower limit but at the fringe of the limit.

Till date, we argued assuming that a new physics will appear at large λ . Is this assumption correct? The large λ may simply mean breakdown of the perturbation theory and may not necessarily guarantee the appearance of new physics. If the perturbative approach fails for $Q > \lambda_{\text{NT}}$, the region $\Lambda_{\text{NT}} < Q < \Lambda$ is where no new physics appears but nonperturbative approach is necessary. Whether such a region exists can be probed using lattice quantum chromodynamics (LQCD). Here, the lattice interval plays the role of the cutoff. Within the lattice QCD formalism, one can perform similar calculations as we did using the perturbation theory, and an upper limit of the Higgs mass was obtained as $m_h < 640$ GeV [18, 19]. It appears that there is no region where the nonperturbative treatment is required. The conclusion we derived using the perturbation theory seems reliable. Therefore, if the Higgs was not found with mass $m_h < 1$ TeV, we could expect new physics nearby. That is, the assumption $m_h \lesssim 1$ TeV seems reasonable. Note, however, $m_h \lesssim 1$ TeV is the theoretical maximum value within reasonable allowance and was not the best guess value. One should remember that predictions of the Higgs, be it phenomenological guess or renormalization group equation argument, pointed to a rather low Higgs mass.

Metastable Vacuum So far we assumed a positive λ , which is necessary for a stable vacuum. However, even if λ goes negative, as long as the vacuum life is longer than the cosmic life time, it is still a viable solution [20]. It is argued that, if the Higgs is light, the vacuum develops an instability below the Planck scale but the EW vacuum is still sufficiently long-lived [21]. The observed value of the Higgs mass ($m_h \sim 125$ GeV, see Section 1.7.6) at LHC is lower than that in Eq. (1.30), which was obtained assuming the vacuum stability within the framework of the SM extrapolated all the way to the Planck scale. Given the LHC mass value, the stability of the EW vacuum has been reevaluated, and the result is shown in Figure 1.6a [8, 22]. Indeed, the quartic coupling constant λ goes negative at large scale, which points to the metastability or instability of the SM vacuum.

The LHC discovery of the Higgs mass ($m_h \simeq 125$ GeV) is at the verge of vacuum metastability. Figure 1.6b shows that the mass value of the Higgs ($m_h = 125 \pm 1$ GeV) points to a position in the metastable region [16, 23, 24]. The stability condition is sensitive also to the value of the top mass and the strong coupling constant α_s . Within the present accuracy ($\Delta m_h = \pm 1$ GeV and $\Delta m_t = \pm 2$ GeV), the allowed region extends both to the stable and the unstable region. A future experiment at the e^-e^+ linear collider (ILC) could reach $\Delta m_h = \pm 50$ MeV, and $\Delta m_t = \pm 200$ MeV, and narrow down the region to the small circle in Figure 1.6b [23].

In summary, the question of the Higgs mass value is an important one directly related to how the new physics will appear. The observation of a Higgs mass of

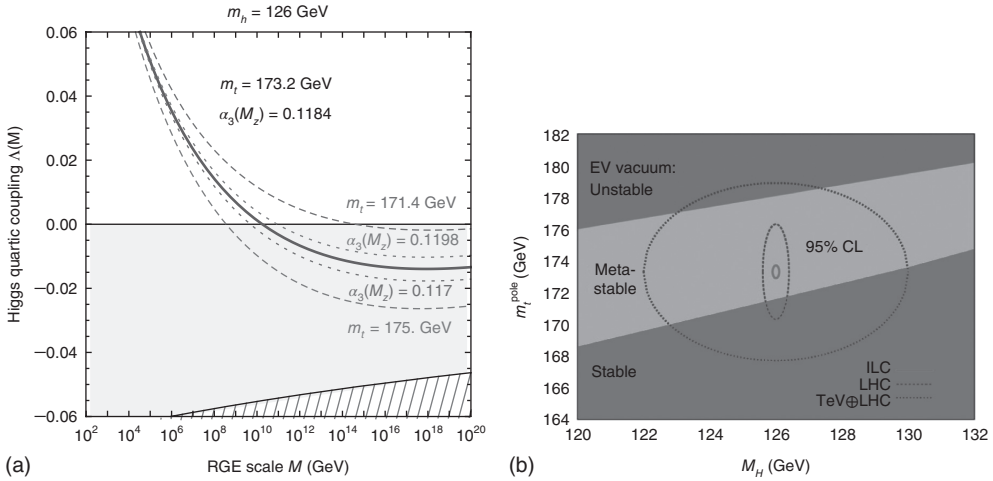


Figure 1.6 (a, b) Renormalization group evolution (RGE) of the Higgs self-coupling for $m_h = 126$ GeV for the central value of m_t and α_s , as well as for $\pm 2\sigma$ variations of m_t (dashed lines) and α_s (dotted lines). For negative values of λ , the lifetime of the SM vacuum due to quantum tunneling at zero temperature is longer than the age of the Universe as long as λ remains above the region shaded in red, which takes into account the finite corrections to the effective bounce action renormalized at the same scale as λ .

(Reproduced with permission of [8, 22].) The 2σ ellipses in the $m_H - m_{\text{top, pole}}$ plane are drawn for the three cases that one obtains from the current top quark and Higgs mass measurements at the Tevatron and LHC, and which can be expected in future measurements at the LHC and at the ILC. The colored area denotes where the SM vacuum is absolutely stable, metastable, and unstable up to the Planck scale. (Reproduced with permission of [16, 23].) (Please find a color version of this figure on the color plates.)

~ 125 GeV would give vacuum stability up to only scales between 10^9 and 10^{10} GeV, and stability up to the Planck scale would require new physics. Such new physics could be the SUSY, but other models have also been discussed [25, 26].

This is the reason why the discovery and the determination of the Higgs mass were so important. As the dynamical properties of the Higgs are directly related to the framework of the SM, it is necessary to know how it is produced. We have to be aware that the production and detection mechanisms differ depending on the mass of the Higgs. They also differ if an e^-e^+ collider is used. We shall review how to produce and detect the Higgs in section 1.7.

1.4 Little and Big Hierarchy Problem

As we emphasized at the beginning of this chapter, the Higgs sector is the least known territory in the SM. All we know is that the gauge symmetry is broken by some VEV referred to as the *Higgs mechanism*. The Higgs Lagrangian in the

SM was chosen for its simplicity, satisfying the minimum requirements for the spontaneous symmetry breaking. We have no idea about the dynamic properties of the Higgs. We do not know whether the Higgs field is an elementary particle, or a composite, or a representation of some dynamical phenomenon. Because of the lack of detailed knowledge of the mechanism of the EW phase transition, the SM loses its predictability for phenomena beyond the teraelectronvolt (TeV) range. It had been expected that new physics would appear at the energy scale of $\sim O(1)$ TeV. However, from the analysis of the electroweak precision data (EWPD) obtained at LEP and Tevatron, reproducibility of the SM is so accurate that any possible deviation due to new physics has to be suppressed by making its cutoff (i.e., energy scale) larger than $\sim O(10)$ TeV. The same EWPD constrains the Higgs mass to be light, ~ 100 GeV with upper limit $m_h < 219$ GeV [7, 27], as we saw in Figure 1.3. Indeed, the mass value of the discovered Higgs turned out to be ≈ 125 GeV. Let us see what problem arises by “the too good SM.”

In the SM, the mass correction to a scalar particle is quadratically divergent because, unlike gauge particles or chiral fermions, there is no known symmetry to suppress the divergence.

Now, if one tries to make corrections to the Higgs mass assuming the validity of the SM up to the energy scale ~ 10 TeV, it gives rise to an unacceptably large Higgs mass value.

This can be seen as follows. There are three types of radiative corrections to the Higgs mass that arose from the diagrams in Figure 1.7a–c.

Each of them gives a correction to the Higgs mass [28]:

$$\text{top loop} \quad -\frac{3}{8\pi^2} Y_t^2 \Lambda^2 \quad \sim -(2 \text{ TeV})^2 \quad (1.39a)$$

$$\text{gauge loop} \quad +\frac{1}{16\pi^2} g^2 \Lambda^2 \quad \sim +(0.7 \text{ TeV})^2 \quad (1.39b)$$

$$\text{Higgs loop} \quad +\frac{1}{16\pi^2} \lambda^2 \Lambda^2 \quad \sim +(0.5 \text{ TeV})^2 \quad (1.39c)$$

The numbers in the third column indicate the values necessary to keep the Higgs mass within the phenomenological limit. If we insert $\Lambda = 10$ TeV in the above expressions, they give

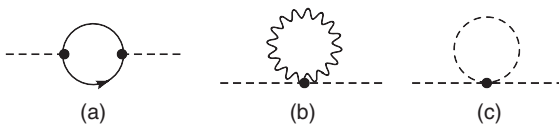


Figure 1.7 Radiative corrections due to the Standard Model. (a) Yukawa coupling with the top quark. (b) Gauge boson loop. (c) Higgs quartic self-interaction.

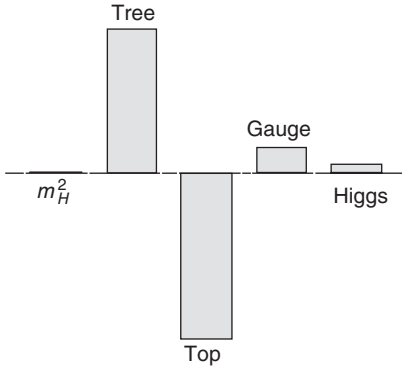


Figure 1.8 Fine-tuning. Three different and large corrections end up with a small Higgs mass.

$$\therefore m_h^2 \simeq m_{\text{tree}}^2 - (100 - 10 - 5) \times (200 \text{ GeV})^2 \quad (1.40)$$

that is, the three large corrections have to conspire to give the small Higgs mass value of ~ 100 GeV. It is a fine-tuning of about 1 part in 100 (see Figure 1.8).

If one avoids the fine-tuning, then one has to limit the energy scale of the new physics below 1–2 TeV. This is referred to as the *little hierarchy problem*. Obviously, the Higgs mass is protected by some kind of symmetry.

The big hierarchy problem appears when one goes to GUTs, that is, if one tries to unify the strong interactions with the EW interactions. As will be discussed in Chapter 3, the grand unification occurs at the energy scale $\sim 10^{16}$ GeV, which is referred to as the *GUT scale*. Extra gauge particles, denoted as X , Y , and Higgs particles denoted as Φ , would also appear.

In the GUTs, the first phase transition occurs at the GUT scale $E_{\text{GUT}} \sim 10^{16}$ GeV and separation of the strong and EW interactions ensue. The second phase transition occurs at the EW scale $E_{\text{EW}} \sim 1/\sqrt{\sqrt{2}G_F} = 246$ GeV, which causes the EW symmetry breakdown of the SM. The extra gauge and Higgs particles acquire masses at the first phase transition.

As energy scale of radiative corrections are generally of the same order as the mass scale of the participating fields, if the Higgs is to fulfill its role of the EW mass generator as an elementary particle, its mass value should be of the order of the EW energy scale. This means that the GUT radiative corrections due to extra gauge bosons X , Y , and heavy Higgs have also to be suppressed to the same scale. This is a fine-tuning to the precision of $(m_{\text{EW}}/m_{\text{GUT}})^2 \sim 10^{28}$. This has to be done at every order of the perturbation expansion that is considered unnatural. The problem is referred to as the *big hierarchy problem* to distinguish it from the little hierarchy problem we have described above.

There are three main approaches to this problem. The first is to introduce a new symmetry, that is, the SUSY, and to try to cancel the diverging radiative corrections order by order by introducing new particles. This is a perturbative

approach, assuming the Higgs to be elementary. The second is to assume that a new strong interaction that breaks the EW symmetry dynamically provides a form factor (i.e., unbinding), with the binding energy playing the role of the cutoff. This is a nonperturbative approach assuming the Higgs to be a composite particle. The third approach is to introduce extra dimensions, a possibility that will be treated in detail in Chapter 6. The second approach generally leads to a heavy Higgs. Therefore, the preferred choice is the first approach. Still, there are models that allow light Higgs (little Higgs model) in the dynamical symmetry-breaking framework.

1.5

Higgs in the Supersymmetry

The SUSY connects fermions and bosons. It introduces a new partner to every particle in the SM. The partners have spins differing by $1/2$ and the same coupling strength such that their additional contributions to the mass corrections cancel those due to the SM partners. The SUSY approach is most attractive because it has nice features in addition to solving the little as well as the big hierarchy problem. By gauging the SUSY, it can produce gravity. Thus, it has the potential to unify all the four forces. Moreover, it is capable of making many definitive predictions that can be tested experimentally. Phenomenologically, it is the most comprehensively studied branch of possible new physics. Details of the SUSY is discussed in Chapters 4 and 5. Here we limit our discussions to its aspect that is specifically related to the Higgs properties.

1.5.1

Two Higgs Doublets

Properties of the Higgs particle in the SM are determined by the Higgs potential. Its form was chosen for its simplicity with minimum requirements, that is, positive quartic coupling $\lambda > 0$, to stabilize the vacuum, and negative quadratic coupling $\mu^2 = -\lambda v^2 < 0$ to induce spontaneous symmetry breaking. So far, there are no observables that contradict this assumption. Besides, the minimum model has been an important guiding principle in exploring the origin and characteristics of spontaneous symmetry breaking theoretically as well as in planning experiments to discover the Higgs particles. However, with EWPD and GUTs in mind, it is important to consider more generic models allowed by phenomenology. There are two important observational constraints in extending the SM.

$$(1) \rho = \frac{G_N}{G_F} = \frac{m_W^2}{m_Z^2 \cos^2 \theta_W} \approx 1.$$

(2) No FCNC (flavor-changing neutral current)

The first is the neutral to charged coupling constant ratio which stays close to unity despite many radiative corrections. A custodial $SU(2)$ symmetry (see Section 3.3.5 of [2]) is believed to be active to protect it. For the second, it is guaranteed by the unitarity of the CKM matrix (Glashow–Iliopoulos–Maiani, GIM, mechanism) in the SM, but if one wants a new physics, an extended GIM mechanism is required.

At the tree level, condition (1) is satisfied automatically if the additional Higgs is a member of doublets (see Eq.(5.12c) of [2]). Therefore, the simplest extension is to require an extra Higgs doublet. The SUSY also requires a minimum of two Higgs doublets. When two Higgs doublets are assumed, there are several ways to satisfy condition (2). The most conventional assumption is to require that one Higgs doublet couples only to up-type quarks (u, c, t) with $Q = +2/3$ and the other only to down-type quarks (d, s, b) with $Q = -1/3$. Let Φ_1, Φ_2 denote two complex $Y = 1, SU(2)$ doublet scalar fields. The most general $SU(2)$ gauge-invariant scalar potential can be written down as [5]

$$\begin{aligned}
 V = & m_{11}^2 \Phi_1^\dagger \Phi_1 + m_{22}^2 \Phi_2^\dagger \Phi_2 - \{ m_{12}^2 \Phi_1^\dagger \Phi_2 + h.c. \} \\
 & + \frac{1}{2} \lambda_1 (\Phi_1^\dagger \Phi_1)^2 + \frac{1}{2} \lambda_2 (\Phi_2^\dagger \Phi_2)^2 + \lambda_3 (\Phi_1^\dagger \Phi_1) (\Phi_2^\dagger \Phi_2) + \lambda_4 (\Phi_1^\dagger \Phi_2) (\Phi_2^\dagger \Phi_1) \\
 & + \left\{ \frac{1}{2} \lambda_5 (\Phi_1^\dagger \Phi_2)^2 + \left[\lambda_6 (\Phi_1^\dagger \Phi_1) + \lambda_7 (\Phi_2^\dagger \Phi_2) \right] \Phi_1^\dagger \Phi_2 + h.c. \right\}
 \end{aligned} \tag{1.41}$$

All the coefficients are real if charge parity (CP) invariance is assumed. We simplify the above potential by imposing the SUSY. In order not to make the arguments too complicated, we adopt the MSSM (minimum supersymmetric extension of the Standard Model) assumption here.

In MSSM, one of the doublets, which we denote as H_1 , has the same quantum number ($Y = -1$) as the charge conjugate of Φ_1 and couples to down-type quarks. The other, denoted as H_2 , has the quantum number of Φ_2 ($Y = +1$) and couples to up-type quarks. As to what the MSSM is, we defer the discussion to Chapter 5. Here we treat the MSSM Higgs potential as given (see Eq. (5.9) [29]). The MSSM relates the coefficients of the quartic potential with the gauge coupling, simplifying the potential to

$$\begin{aligned}
 V_H = & \mu_1^2 H_1^\dagger H_1 + \mu_2^2 H_2^\dagger H_2 - \mu_3^2 (\epsilon_{ij} H_1^i H_2^j + h.c.) \\
 & + \frac{g_W^2 + g_B^2}{8} (H_1^\dagger H_1 - H_2^\dagger H_2)^2 + \frac{g_W^2}{2} |H_1^\dagger H_2|^2
 \end{aligned} \tag{1.42}$$

where $\epsilon_{12} = -\epsilon_{21} = 1$, $\epsilon_{11} = \epsilon_{22} = 0$ and H_1^i, H_2^j are components of the Higgs doublet H_1 and H_2 . g_W, g_B are the gauge coupling constants of $SU(2)_L$ and $U(1)_Y$, respectively. As H_1^c and H_2 have the same quantum number, we define two complex

neutral and two charged scalar fields by

$$H_1 = \begin{bmatrix} H_1^1 \\ H_1^2 \end{bmatrix} = \Phi_1^c = \begin{bmatrix} \phi_1^{0+} \\ -\phi_1^- \end{bmatrix} \quad \text{8)} \quad (1.43a)$$

$$H_2 = \begin{bmatrix} H_2^1 \\ H_2^2 \end{bmatrix} = \Phi_2 = \begin{bmatrix} \phi_2^+ \\ \phi_2^0 \end{bmatrix} \quad (1.43b)$$

Then, the potential Eq. (1.42) is rewritten as follows:

$$\begin{aligned} V_H = & \mu_1^2(|\phi_1^0|^2 + |\phi_1^-|^2) + \mu_2^2(|\phi_2^0|^2 + |\phi_2^+|^2) - \mu_3^2(\phi_1^{0+}\phi_2^0 + \phi_1^-\phi_2^+ + h.c.) \\ & + \frac{g_W^2 + g_B^2}{8} (|\phi_1^0|^2 + |\phi_1^-|^2 - |\phi_2^0|^2 - |\phi_2^+|^2)^2 + \frac{g_W^2}{2} |\phi_1^{0+}\phi_2^+ - \phi_1^+\phi_2^0|^2 \end{aligned} \quad (1.46)$$

To break the symmetry spontaneously, we choose the VEVs to satisfy $\langle \phi_1^+ \rangle = \langle \phi_2^- \rangle = 0$ so that the charge conservation is respected. Then, to obtain the final VEV, it is enough to consider only the neutral fields. We assume that the minimum of the potential is at

$$\langle H_1^c \rangle = \begin{bmatrix} 0 \\ \frac{v_1}{\sqrt{2}} \end{bmatrix}, \quad \langle H_2 \rangle = \begin{bmatrix} 0 \\ \frac{v_2}{\sqrt{2}} \end{bmatrix} \quad (1.47)$$

There are two important conditions for the potential:

- (1) For the vacuum stability, the potential has to be bound from below. For $|\phi_1^0| \neq |\phi_2^0|$, it is automatic, but for $|\phi_1^0| = |\phi_2^0|$, one needs a condition $\mu_1^2 + \mu_2^2 > 2\mu_3^2$.
- (2) To obtain symmetry breaking, the coefficient of the quadratic term must be negative, which amounts to $\mu_3^4 > \mu_1^2\mu_2^2$.

The minimum of the potential can be obtained by substituting $\phi_1^0 = v_1/\sqrt{2}$, $\phi_2^0 = v_2/\sqrt{2}$ in the potential and requiring $\partial V_H/\partial v_1 = \partial V_H/\partial v_2 = 0$. We obtain two

- 8) This way of arranging the Higgs doublets may strike odd for those who are accustomed to the four-component Dirac spinor representation. Indeed, in [1] and [2] of this book (and also in Equation (1.7)), the Yukawa interaction to give mass to a quark doublet is arranged as follows:

$$\begin{aligned} -\mathcal{L}_{\text{Yukawa}} = & \gamma_d(\bar{\Psi}_L\Phi)d_R + \gamma_u(\bar{\Psi}_L\Phi_c)u_R + h.c. \\ \Psi_L = & \begin{bmatrix} u_L \\ d_L \end{bmatrix}, \quad \Phi = \begin{bmatrix} \phi^+ \\ \phi^0 \end{bmatrix}, \quad \Phi_c = \begin{bmatrix} \phi^{0+} \\ -\phi^- \end{bmatrix} \end{aligned} \quad (1.44)$$

The reason why the Higgs fields are expressed like Eq. (1.43) is because, in the supersymmetric formalism, two-component left-handed Weyl spinors are the preferred bases to express fermion fields. Both quark and Higgs doublets are in the left-handed representation. The SU(2) invariant made of two doublets is expressed as (see Appendix A of [1])

$$\begin{aligned} -\gamma_u(u_R)^c \varepsilon_{ij} q_L^i H_2^j + \gamma_d(d_R)^c \varepsilon_{ij} q_L^i H_1^j, \\ (q_L^1, q_L^2) = (u_L, d_L), \quad \varepsilon_{12} = -\varepsilon_{21} = -1 \end{aligned} \quad (1.45)$$

Thus, the position of the neutral component in the Higgs doublets should be reversed to produce the correct mass terms when they get the vacuum expectation value.

relations as

$$\begin{aligned}\mu_1^2 &= \mu_3^2 \frac{v_2}{v_1} - \frac{1}{8}(g_W^2 + g_B^2)(v_1^2 - v_2^2) = \mu_3^2 \tan \beta - \frac{m_Z^2}{2} \cos 2\beta \\ \mu_2^2 &= \mu_3^2 \frac{v_1}{v_2} + \frac{1}{8}(g_W^2 + g_B^2)(v_1^2 - v_2^2) = \mu_3^2 \cot \beta + \frac{m_Z^2}{2} \cos 2\beta\end{aligned}\quad (1.48)$$

where the important angle β is defined by

$$\tan \beta \equiv \frac{v_2}{v_1} \quad (1.49)$$

The VEV of the SM, $v^2 \equiv v_1^2 + v_2^2$, is fixed by the relation $m_W = g_W v/2$, which leads to the second equality in Eqs. (1.48). The Z mass-squared, in turn, is given by

$$m_Z^2 = \frac{\mu_1^2 - \mu_2^2 \tan^2 \beta}{\tan^2 \beta - 1} \quad (1.50)$$

One sees that the two equations in Eq. (1.48) automatically satisfy the vacuum stability and the symmetry-breaking conditions.

1.5.2

Coupling Strengths of MSSM Higgs

As the SUSY relates the gauge sector to the Higgs sector, the coupling of the Higgs is uniquely determined once the SUSY parameters ($\tan \beta$, $\tan \alpha$) are given. α is the mixing angle of neutral Higgs fields and is given by Eq. (1.63). As it is lengthy to write down all the interactions, we list a few in Tables 1.1–1.4 [4, 30] to illustrate the constraints imposed by the SUSY.

Here, φ_{SM} denotes the Higgs in the SM.

The coupling of the charged Higgs to the fermion is given by

$$\mathcal{L}_{\text{INT}} = \frac{g_W}{2\sqrt{2}m_W} \bar{t} \left[m_t \cot \beta (1 + \gamma^5) + m_b \tan \beta (1 - \gamma^5) \right] b H^+ + h.c. \quad (1.51)$$

This equation is written in terms of (t, b) , but couplings to other fermions can be written down similarly. The couplings being specified, all the remaining parameters are the masses of the particle. Therefore, the production cross section, and hence the detection method, can be determined once the mass value is specified.

Table 1.1 Coupling strength of the neutral Higgs to the fermion.

$$\mathcal{L}_{\text{INT}} \sim -\frac{g_W}{2} \frac{m_f}{m_W} \bar{f} O_i f \phi_i$$

ϕ_i		h^0	H^0	A	φ_{SM}
O_i	$f = t$	$\frac{\cos \alpha}{\sin \beta}$	$\frac{\sin \alpha}{\sin \beta}$	$-i\gamma^5 \cot \beta$	1
	$f = b$	$-\frac{\sin \alpha}{\cos \beta}$	$\frac{\cos \alpha}{\cos \beta}$	$-i\gamma^5 \tan \beta$	1

Table 1.2 Coupling strength of the neutral Higgs to the vector boson.
$$\mathcal{L}_{\text{INT}} \sim ig_V m_V O_i g_{\mu\nu} V_\mu V^\nu \phi_i$$

$$(g_W = e/\sin\theta_W, g_Z = e/\sin\theta_W \cos\theta_W)$$

ϕ_i	h^0	H^0	A	φ_{SM}
O_i	$-\sin(\alpha - \beta)$	$\cos(\alpha - \beta)$	0	1

Table 1.3 Coupling strength of the neutral CP-odd Higgs to the vector boson.
$$\mathcal{L}_{\text{INT}} \sim V\phi(p)\phi(p') \sim \frac{g_Z}{2} O_i (p - p')^\mu Z_\mu A^0 \phi_i$$

ϕ_i	h^0	H^0	φ_{SM}
O_i	$\cos(\alpha - \beta)$	$-\sin(\alpha - \beta)$	0

Table 1.4 Coupling strength of the charged Higgs to the vector boson.
$$\mathcal{L}_{\text{INT}} \sim V\phi(p)\phi(p') \sim -i\frac{g_W}{2} O_i (p - p')^\mu W_\mu^\pm H^\mp \phi_i$$

ϕ_i	h^0	H^0	φ_{SM}
O_i	$\cos(\alpha - \beta)$	$\sin(\alpha - \beta)$	0

We give a partial list of allowed and forbidden couplings at the tree level. The radiative corrections modify them, but they are omitted.

$$\begin{aligned} \circ : & [VVH^0, VVh^0], [ZA^0H^0, ZA^0h^0], ZH^+H^-, [W^\pm H^\mp H^0, W^\pm H^\mp h^0] \\ & [ZZH^0, ZZh^0], \dots \\ \times : & VVA^0, ZW^\pm H^\mp, ZH^0h^0, ZH^0H^0, Zh^0h^0, ZA^0A^0, \dots \end{aligned} \quad (1.52)$$

The coupling of the pair in the $[\dots]$ is like $\sim [\sin x, \cos x]$ and complementary in the sense that, if one is smaller, the other is larger. The complementarity is related to the unitarity. In a theory where the symmetry is spontaneously broken, processes containing the Higgs have a role to compensate a class of diverging integrals (see discussions in Chapter 1 of [2]). For example, if a process in which both H^0, h^0 are exchanged contributes to compensation of diverging WW integrals, the combined effect of the H^0, h^0 has to be the same as the SM's Higgs which constrains the relation between the two. That is,

$$g^2(h^0 WW) + g^2(H^0 WW) = g_W^2 \quad (1.53)$$

Referring to Table 1.2, one sees that the above equation is satisfied. Furthermore, we also have

$$g^2(h^0 ZZ) + g^2(H^0 ZZ) = g_Z^2 \quad (1.54a)$$

$$g^2(h^0 A^0 Z) + g^2(H^0 A^0 Z) = g_Z^2 \quad (1.54b)$$

These considerations mean that one of A^0, h^0, H^0 has a detection probability similar to that of the SM Higgs.

1.5.3

Mass Spectrum of MSSM Higgs

Spontaneous breakdown of the symmetry induces mixing and changes the mass eigenvalues. Out of eight scalar fields, three are taken up by the gauge bosons to give them mass, and five appear as physical particles. Three of them are neutral and the rest two are charged. If the CP invariance is assumed, the real and imaginary parts of the scalar fields do not mix and the charged Higgs's are also separated. Let us derive the mass of the CP-odd neutral scalar first. By extracting terms quadratic in $\text{Im } \phi_1^0$ and $\text{Im } \phi_2^0$, we obtain the following mass matrix:

$$M_A^2 = \mu_3^2 \times (\text{Im } \phi_1^0, \text{Im } \phi_2^0) \begin{bmatrix} \frac{v_2}{v_1} & -1 \\ -1 & \frac{v_1}{v_2} \end{bmatrix} \begin{pmatrix} \text{Im } \phi_1^0 \\ \text{Im } \phi_2^0 \end{pmatrix} \quad (1.55)$$

As the determinant vanishes, one eigenvalue is 0 corresponding to the would-be-Goldstone boson which was eaten by the Z boson.⁹ The other corresponds to a CP-odd neutral scalar field, which we denote as A. By diagonalizing the mass matrix, we obtain masses and expressions for the field A as well as the would-be-Goldstone field G^0 .

$$m_A^2 = \mu_3^2 (\tan \beta + \cot \beta) = \frac{2\mu_3^2}{\sin 2\beta} \quad (1.56)$$

$$A = \sqrt{2} (-\text{Im } \phi_1^0 \sin \beta + \text{Im } \phi_2^0 \cos \beta), \quad (1.57a)$$

$$G^0 = \sqrt{2} (\text{Im } \phi_1^0 \cos \beta + \text{Im } \phi_2^0 \sin \beta) \quad (1.57b)$$

The mass matrix of the charged Higgs can be obtained similarly.

$$\begin{aligned} M_{H^\pm}^2 &= \left(\frac{\mu_3^2}{v_1 v_2} + \frac{g_W^2}{4} \right) \times (\phi_1^+, \phi_2^+) \begin{bmatrix} v_2^2 & -v_1 v_2 \\ -v_1 v_2 & v_1^2 \end{bmatrix} \begin{pmatrix} \phi_1^- \\ \phi_2^- \end{pmatrix} \\ &= (m_A^2 + m_W^2) \times (\phi_1^+, \phi_2^+) \begin{bmatrix} \sin^2 \beta & -\sin \beta \cos \beta \\ -\sin \beta \cos \beta & \cos^2 \beta \end{bmatrix} \begin{pmatrix} \phi_1^- \\ \phi_2^- \end{pmatrix} \end{aligned} \quad (1.58)$$

where we used Eq. (1.49) and (1.56) in going to the second line. Again, one of the masses vanishes. The other mass has a finite eigenvalue and is physical. They are related by

$$m_{H^\pm}^2 = m_A^2 + m_W^2 \quad (1.59)$$

$$H^\pm = -\phi_1^\pm \sin \beta + \phi_2^\pm \cos \beta, \quad G^\pm = \phi_1^\pm \cos \beta + \phi_2^\pm \sin \beta \quad (1.60)$$

9) The Goldstone bosons that are absorbed by gauge particles are referred to as the *would-be-Goldstone bosons*, and physical Goldstone bosons that acquire mass through additional external force are referred to as the *pseudo Nambu-Goldstone bosons* (pNGBs) to distinguish them from the zero-mass Goldstone bosons.

In order to obtain the mass matrix of the two CP-even neutral Higgs particles, we set $\phi_1^0 = v_1/\sqrt{2}$, $\phi_2^0 = v_2/\sqrt{2}$, $\phi_1^\pm = \phi_2^\pm = 0$ and calculate

$$\begin{aligned} M_{\text{CP}^+}^2 &= \frac{1}{2} \left. \frac{\partial^2 V_H}{\partial v_i \partial v_j} \right|_{v_i, v_j=0} = \begin{bmatrix} \mu_3^2 \tan \beta + m_Z^2 \cos^2 \beta & -\mu_3^2 - m_Z^2 \sin \beta \cos \beta \\ -\mu_3^2 - m_Z^2 \sin \beta \cos \beta & \mu_3^2 \cot \beta + m_Z^2 \sin^2 \beta \end{bmatrix} \\ &= \begin{bmatrix} m_A^2 \sin^2 \beta + m_Z^2 \cos^2 \beta & -\frac{1}{2}(m_A^2 + m_Z^2) \sin 2\beta \\ -\frac{1}{2}(m_A^2 + m_Z^2) \sin 2\beta & m_A^2 \cos^2 \beta + m_Z^2 \sin^2 \beta \end{bmatrix} \end{aligned} \quad (1.61)$$

Diagonalizing the mass matrix, we obtain

$$m_{H,h}^2 = \frac{1}{2} \left[m_A^2 + m_Z^2 \pm \sqrt{(m_A^2 + m_Z^2)^2 - 4m_Z^2 m_A^2 \cos^2 2\beta} \right] \quad (1.62)$$

It is customary to denote the heavier one of the two mass eigenstates as H^0 and the lighter one as h^0 . They are given by

$$H^0 = \left(\sqrt{2} \text{Re} \phi_1^0 - v_1 \right) \cos \alpha + \left(\sqrt{2} \text{Re} \phi_2^0 - v_2 \right) \sin \alpha \quad (1.63a)$$

$$h^0 = -\left(\sqrt{2} \text{Re} \phi_1^0 - v_1 \right) \sin \alpha + \left(\sqrt{2} \text{Re} \phi_2^0 - v_2 \right) \cos \alpha \quad (1.63b)$$

$$\tan 2\alpha = \frac{m_A^2 + m_Z^2}{m_A^2 - m_Z^2} \tan 2\beta, \quad -\frac{\pi}{2} \leq \alpha \leq 0 \quad (1.63c)$$

From the above equations, we have the relations

$$\begin{aligned} m_{H^\pm}^2 &> m_W^2 \\ m_{H^0} &> \max(m_A, m_Z) \geq \min(m_A, m_Z) \cos 2\beta \geq m_h \\ m_h^2 + m_{H^0}^2 &= m_Z^2 + m_A^2 \end{aligned} \quad (1.64)$$

Thus, the supersymmetric structure of the theory has imposed very strong conditions on the Higgs spectrum. Out of six parameters that describe the MSSM Higgs sector $(m_h, m_H, m_A, m_{H^\pm}, \beta, \alpha)$, only two parameters that can be taken as $\tan \beta$ and m_A are free parameters at the tree level.

The relations Eqs. (1.64) mean that at least one of the three neutral Higgs particles is lighter than Z. Therefore, if one can prove the existence of a light Higgs h^0 with mass smaller than Z, the possibility of the SUSY, or at least its minimum version MSSM, is very large. Notice, however, that this story is valid only for the tree approximation. Inclusion of radiative corrections modifies the mass value, especially those including the massive top and its spin 0 partner ‘‘stop’’ quark. The correction to the light Higgs mass is given by [31–34] [30, 35]

$$\begin{aligned}
m_h^2 &\rightarrow m_h^2 + \delta m_h^2 \\
&\simeq m_Z^2 + \frac{3}{2\pi^2} \left(\frac{m_t^4}{v^2} \right) \left[\ln \left(\frac{M_S^2}{m_t^2} \right) + \frac{X_t^2}{M_S^2} \left(1 - \frac{X_t^2}{12M_S^2} \right) \right]^{10}
\end{aligned} \tag{1.65}$$

where $X_t = A_t - \mu \cot \beta$ is the mixing parameter in the stop sector [see Eq. (5.35)]. We have characterized the scale of “stop” (\tilde{t}_1, \tilde{t}_2) masses with $M_S \equiv (m_{\tilde{t}_1} m_{\tilde{t}_2})^{1/2}$.

Figure 1.9 shows the values of corrected m_h as well as m_{H^0} , m_{H^\pm} as a function of m_A for two values of $\tan \beta = 3, 30$ with the maximum mixing scenario. m_h almost saturates and is insensitive to $\tan \beta$ or m_A whether they take values larger than those given in Figure 1.9. Thus one sees that, even after the radiative corrections, the mass of the light Higgs remains relatively small, $m_h \lesssim 120 \sim 140$ GeV. The existence of the light Higgs is a solid prediction of the SUSY. The mass value ($m_h = 125.7 \pm 0.4$ GeV) determined by LHC is near the upper limit of the SUSY predictions. It means that parameters of the MSSM to reproduce the observed value are near the boundaries of allowed regions. The stop mass, in particular, takes a large value (\gtrsim a few tetraelectron volts) in the conventional scenario of the MSSM [36].

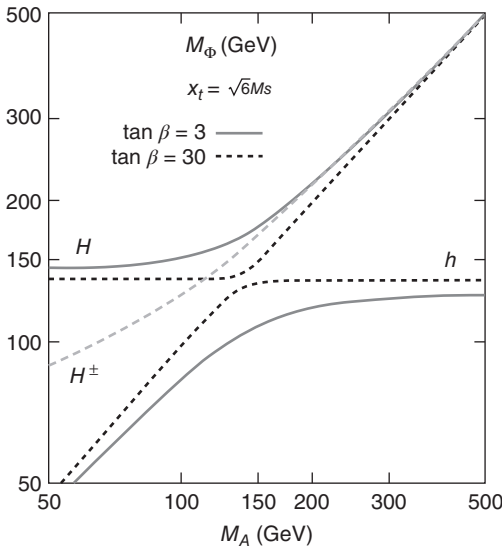


Figure 1.9 Mass of the MSSM Higgs bosons as functions of m_A for two values of $\tan \beta = 3, 30$ with maximal mixing scenario with the stop (\tilde{t}) mass $m_{\tilde{t}} = 2$ TeV and all other SUSY parameters set to 1 TeV. (Reproduced with permission of [30].)

10) There are two “stop” mass eigenstates \tilde{t}_1, \tilde{t}_2 that are obtained by the mixing of \tilde{t}_L, \tilde{t}_R , which are super partners of the top (t_L, t_R). M_S is defined as the geometric mean of the two stop masses ($M_S = \sqrt{m(\tilde{t}_1)m(\tilde{t}_2)}$). The mixing is induced by the Yukawa coupling of the Higgs to both particles.

In the SM, the Higgs mass is basically a free parameter. In the MSSM model, however, the light Higgs (h) is bounded from above with its mass given by Eq. (1.65). This is obtained in the so-called decoupling regime where the value of m_A is set high, pushing masses of other Higgses (H^0 , H^\pm) high also. This is a scenario to maximize m_h in the framework of SUSY. An analysis of the Higgs mass guided by the naturalness condition (i.e., no excessive fine tuning) is shown in Figure 1.10a. One sees that a large mixing (large $A_t - \mu \cot \beta$, see Eqs. (1.65), (5.35)) as well as a large stop mass is required to realize the observed value of the Higgs. As the lighter stop is considered as the lightest of all squarks, it means that other squark masses are at least higher than $\sim 700\text{GeV}$, consistent with direct search results. The difference of the two curves in the figure (Suspect and FeynHiggs) may be considered as the theoretical uncertainty. Validity of various SUSY models was also examined and is shown in Figure 1.10b. The observed Higgs mass value excludes the GMSB (gauge mediated symmetry breaking) and AMSB (anomaly mediated symmetry breaking) in their simplest version. They will be discussed in Section 5.4 and 5.5. For no or small mixing, a much higher value of M_S is required. The limit of $M_S < 3\text{ TeV}$ may be set from naturalness consideration. If one removes the constraint on these models, freedom of realizing the observed mass increases, and many alternative models are being discussed.

In the high scale SUSY, for instance, the mass scale of all the SUSY particles are set high, while in the split SUSY [40–42], only the scalars (squarks and sleptons) are pushed beyond the LHC reach ($\sim 10^9\text{ GeV}$). Figure 1.11 shows the predicted range of the Higgs mass [16]. However, fermions, that is, gauginos and higgsinos, remain at the low energy scale. One conspicuous feature of the split SUSY is a long-lived

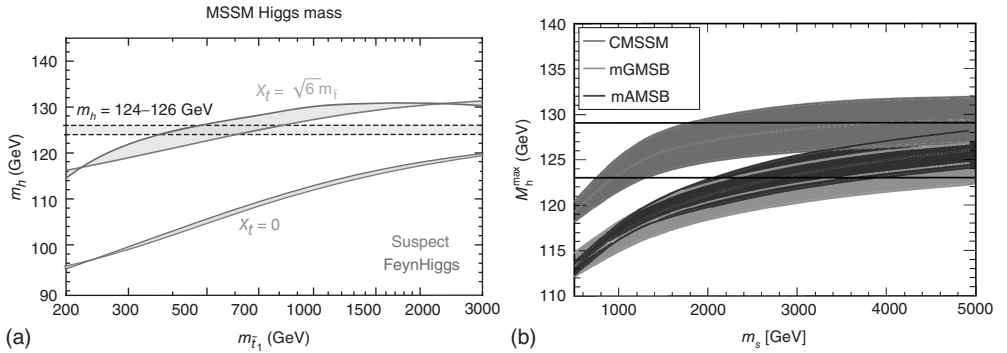


Figure 1.10 (a) Higgs mass as a function of the scalar top mass. Other SUSY parameters were fixed at values guided by naturalness conditions. Large mixing and stop mass are required. (Reproduced with permission of [37].) (b) The Higgs mass shown as a function of $M_S = (m_{\tilde{t}_1} m_{\tilde{t}_2})^{1/2}$ for the various constrained MSSM models. Note

that, for reasonable values of $M_S \lesssim 3000\text{ GeV}$, simple versions of GMSB, AMSB are ruled out. CMSSM (constrained minimum supersymmetric extension of the Standard Model discussed in Section 5.3) survives. (Reproduced with permission of [38, 39].) (Please find a color version of this figure on the color plates.)

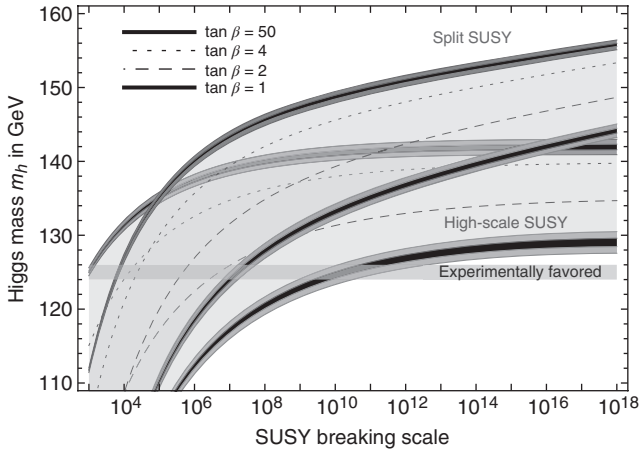


Figure 1.11 NNLO prediction for the Higgs mass m_h in high-scale supersymmetry (blue, lower) and split supersymmetry (red, upper) for $\tan\beta = \{1, 2, 4, 50\}$. The thickness of the lower boundary at $\tan\beta = 1$ and of the upper boundary at $\tan\beta = 50$ shows the uncertainty due to the present 1σ error on α_s (black band) and on the top mass (larger colored band). (Reproduced with permission of [16].) (Please find a color version of this figure on the color plates.)

gaugino, which could have lifetime as long as 100 s [43, 44]. This is because the gluino’s decay has to go through the heavy squark loops. However, the split SUSY retains basic virtues of the SUSY, that is, gauge unification (see Section 3.6), the dark matter candidate and possibly the light SM-like Higgs boson [45].

In summary, the mass of the Higgs is still within the allowed limit of the MSSM, but many parameters are pushed almost to their extreme limits, thereby excluding many of the more constrained models.

1.6

Is the Higgs Elementary?

So far, we treated the Higgs as an elementary particle. Notice, however, that the Higgs mechanism was constructed using superconductivity as a model. In superconductivity, spontaneous symmetry breaking is induced by the Cooper pair, which is a composite of two electrons. In QCD, chiral symmetry breaking is induced by the condensate of the quark–antiquark pair. It is quite logical to think that the Higgs may also be a composite. In this case, one considers a new, strong interaction which works among new particles and regards the Higgs as a bound state of some particle pairs.¹¹⁾ Representative models are the technicolor (TC) model and, more recently, the little Higgs model.

¹¹⁾ One does not necessarily introduce new particles or new interactions. For instance, the top condensate model considers the Higgs as a bound state of top and anti-top quarks [46–48].

1.6.1

Technicolor Model

A representative theory of the strong dynamical symmetry breaking is the TC model [49–52]. Just like the pion is the NGB, which emerges from the chiral symmetry breaking ($SU(2)_L \times SU(2)_R \rightarrow SU(2)_V$) as a result of the $\bar{q}q$ condensation in QCD, the Higgs can also be considered as the NGBs of the new gauge symmetry $SU(N_{TC})$ with new fermions (techni-fermions)

$$\Psi_L = \begin{bmatrix} U \\ D \end{bmatrix}_L, \quad U_R, \quad D_R \quad (1.66)$$

constituting the fundamental representation. If $N_{TC} = 3$, one may consider TC as the scaled-up version of QCD = color $SU(3)$. For simplicity, however, we consider $N_{TC} = 1$, with only two flavors (U, D). Generalization to $N_{TC} > 1$ can be done easily. The fermion kinetic energy terms for this theory are

$$\mathcal{L}_{\text{kin}} = \bar{\Psi}_L i D_\mu \gamma^\mu \Psi_L + \bar{U}_R i D_\mu \gamma^\mu U_R + \bar{D}_R i D_\mu \gamma^\mu D_R \quad (1.67)$$

and like QCD, they have a chiral $SU(2)_L \times SU(2)_R$ symmetry in the $m_U = m_D = 0$ limit. The gauge boson is referred to as the *techni-gluon*, and the interaction by exchange of the techni-gluon induces the formation of a condensate

$$\langle \bar{U}_L U_R \rangle = \langle \bar{D}_L D_R \rangle \simeq F_{TC}^3 \quad (1.68)$$

which dynamically breaks the gauge symmetry $SU(2)_L \times SU(2)_R \rightarrow SU(2)_V$. Just like the QCD, the NGBs appear as the techni-pions ($\pi_{TC}^+, \pi_{TC}^0, \pi_{TC}^-$) = $[\bar{D}U, (\bar{U}U - \bar{D}D)/\sqrt{2}, \bar{U}D]$, which are absorbed by the gauge bosons of the EW interaction.¹²⁾ When there are N_D techni-fermion doublets, the constant F_{TC} is modified to [52]

$$F_{TC} \simeq \frac{v_0}{\sqrt{N_D}}, \quad v_0 = 246 \text{ GeV} \quad (1.69)$$

for $N_D = 1$ $F_{TC} = v_0$. In QCD, the VEV of the quark condensate is related to the pion decay constant F_π by the relation

$$\langle \bar{u}_L u_R \rangle \simeq \langle \bar{d}_L d_R \rangle \simeq F_\pi^3 \quad (1.70)$$

$$F_\pi = 96 \text{ MeV}$$

Therefore, TC is a scaled-up QCD by a factor of

$$\frac{F_{TC}}{F_\pi} = \frac{246 \text{ GeV}}{96 \text{ MeV}} \approx 2500 \quad (1.71)$$

If the chiral symmetry is larger than $SU(2)_L \times SU(2)_R$, it will contain extra NGBs which are not eaten by the gauge particles. They will acquire mass (referred to as *pseudo-Nambu-Goldstone boson*, *pNGB*) due to the nonzero techni-fermion mass, just

12) Notice that, in the simplest model, they have spin parity 0^- . If the observed Higgs has spin parity 0^+ , one has to think of a p-wave excited state to assign the NGB boson to the Higgs. This is another complication of the TC model.

like $SU(3)_{\text{flavor}}$ octet NGBs are massive in QCD. While the Higgs may not appear in TC, it is likely that the strongly interacting pNGBs form a variety of resonances ($\rho_{\text{TC}}/\omega_{\text{TC}}, a_{\text{TC}}, \text{etc.}$),¹³⁾ just like the $\pi\pi$ pair forms the vector resonance $\rho/\omega/a_1$. In such a case, a rich spectra of new particles will appear above the TeV region.

Extended technicolor: The basic idea of the TC is very attractive and solves the fine-tuning problem by providing a natural cutoff (i.e., form factor of the bound states) for the high-energy part of the radiative contributions. However, realistic models have to reproduce the mass spectra of known fermions and phenomenologically established constraints, that is, suppression of FCNC. The mass generation mechanism of the ordinary fermions (denoted as f) is through Yukawa coupling in the SM, but the Higgs in TC is a composite of the technifermions. In order to generate the fermion mass, one has to have a new interaction that couples both to ordinary and TC fermions. The standard choice is the ETC (extended technicolor), a new gauge interaction at higher energy scale than the typical TC energy, which is of the order of the EW symmetry breaking. Exchange of the ETC gluon provides the fermion–fermion interaction and generates an effective mass. On the other hand, the same ETC interaction produces the FCNC interaction, and it is hard to construct a phenomenologically viable model. A remedy is the walking TC model, which assumes that the gauge coupling α_{TC} evolves slowly (i.e., it walks, not runs).

While the TC model itself is on a tightrope phenomenologically, we emphasize that the notion of the dynamical symmetry breaking is a viable one [52]. Therefore, we look for possible signals of the TC in the LHC data. Analyses are inevitably model-dependent. We show below those based on the LSTC (low-scale technicolor) model by [53, 54]. Here, the lightest techni-hadron is the techni-pion π_{TC} . The next lightest are $\rho_{\text{TC}}, \omega_{\text{TC}},$ and $a_{1\text{TC}}$, which are almost degenerate.

Experimental searches: The CMS group looked for the TC particles that would appear as an excess in WZ channels [55]. The main interest was to find $\rho_{\text{TC}}/a_{\text{TC}} \rightarrow WZ$ as well as $W' \rightarrow WZ$, where W' is a heavy W which appears in a variety of models¹⁴⁾. But, here we concentrate on $\rho_{\text{TC}}/a_{\text{TC}}$ signals which are collectively called ρ_{TC} , as they cannot be distinguished in the WZ channel. Signals are $X \rightarrow 3l + \nu$.

Figure 1.12a shows their accumulated number of events as a function of the WZ invariant mass. Formally, the invariant mass of WZ cannot be uniquely determined. However, by assuming the W to have its nominal mass, the value of the neutrino longitudinal momentum is constrained to one of the two solutions of a quadratic equation. According to Monte Carlo simulations, the smaller of the two turned out to be the right solution 75% of the time and this solution was adopted for all events. The parameter $\sin \chi$ they used is given by [56]

$$\sin \chi = \frac{F_{\text{TC}}}{v_0} = \frac{F_{\text{TC}}}{246} \text{ GeV} \approx \frac{1}{\sqrt{N_D}} \ll 1 \quad (1.72)$$

13) $I^G(J^{PC})$ of $\pi_{\text{TC}}, \rho_{\text{TC}}, \omega_{\text{TC}}, a_{1\text{TC}}$ are $1^-(0^{++}), 1^+(1^{--}), 0^-(1^{--}),$ and $1^-(1^{++})$.

14) Conventionally, it is assumed to have identical coupling strength as the SM W , which is referred to as the *Sequential Standard Model* (SSM).

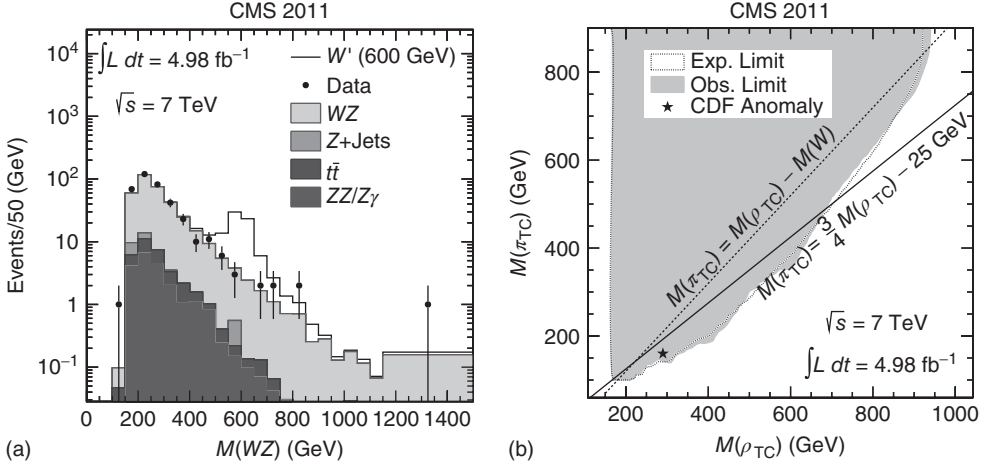


Figure 1.12 (a) Distribution of the WZ invariant mass. W' in SSM with mass point at 600 GeV is denoted as a white histogram. (b) Exclusion region at 95% CL for the LSTC (low-scale TC) model as a function of ρ_{TC} and π_{TC} masses. (Reproduced with permission of [55].)

The data agreed with the SM prediction, and no signal of TC resonances was obtained. The right figure of Figure 1.12b shows the excluded region on the $M(\pi_{TC}) - M(\rho_{TC})$ plane. TC hadrons (ρ_{TC} etc.) with masses between 167 and 687 GeV have been excluded, assuming $M(\pi_{TC}) = (3/4)M(\rho_{TC}) - 25 \text{ GeV}$. The region $M(\pi_{TC}) > M(\rho_{TC})$ is theoretically forbidden.

The ATLAS group, in their search for TC in dilepton decay channels, obtained similar results [57].

1.6.2

Little Higgs Model

An alternative to the TC model recently being discussed is the “little Higgs model” [28, 58]. Like TC, it considers the Higgs as an Nambu Goldstone Boson (NGB) produced by the spontaneously broken symmetry of a new, strong force [59, 60]. But unlike TC, which introduces a new force explicitly, it focuses on global symmetry breaking, though the new interaction is implicit by its NGB assumption. It also retains the light Higgs, and is thus more realistic phenomenologically.

Denoting the global symmetry as G , it must include the EW symmetry ($G \supset SU(2) \times U(1)$). Being the NGB, the Higgs is massless at the tree level. By treating it in the framework of the nonlinear σ model (see the boxed paragraph and also Appendix J of [2]), one can construct an effective theory of a new, strong interaction which recovers the SM in the low-energy limit.

The nonlinear σ model expresses the Nambu-Goldstone boson (NGB) as a phase field analogous to Eq. (1.12).

$$\Sigma = \sigma + i\boldsymbol{\tau} \cdot \boldsymbol{\pi} \rightarrow (v + \rho)e^{i\boldsymbol{\pi} \cdot \boldsymbol{\tau}/2v} = (v + \rho)U \quad (1.73)$$

where σ (or ρ after symmetry breakdown) is a scalar field which induces spontaneous symmetry breakdown and $\boldsymbol{\pi}$ are the NGBs associated with broken symmetry (in this case the global symmetry is $SU(2)$ chiral symmetry). In this expression, the phase transformation for $\boldsymbol{\pi}$ becomes the shift transformation, and hence the gauge invariance allows only derivative couplings for $\boldsymbol{\pi}$. Therefore, the zero mass at the tree level is automatic. The Lagrangian is expanded in powers of field derivatives but otherwise constrained only by the symmetry.

$$\mathcal{L}_{\text{eff}} = \frac{v^2}{4} \text{Tr}[\partial_\mu U \partial^\mu U^\dagger] + \frac{v^2}{8m_\rho^2} (\text{Tr}[\partial_\mu U \partial^\mu U^\dagger])^2 + \dots \quad (1.74)$$

As the field derivatives are momenta, the first few terms give an effective low-energy ($\sqrt{s} \ll m_\rho$) Lagrangian.

Therefore, the starting point is a scaled-up chiral perturbation theory in which the pion is replaced with the Higgs. The lightness of the pion mass is due to its identity being the NGB. The Higgs as the NGB can acquire mass if the global symmetry G is explicitly broken. This is achieved by converting the derivative to a covariant derivative (i.e., by gauging), because the gauge interaction induces the quadratic (i.e., mass term) as well as the quartic field configuration radiatively [6]. If the whole or part of the gauged symmetry contains the EW symmetry, one can fulfill the aim to reproduce the SM as a low-energy effective theory.

The challenge, then, is to fulfill the requirement that the new strong force should only appear beyond the energy scale $\sim O(10)$ TeV while keeping the Higgs mass light. Let us rephrase the problem in more technical terms. Major corrections to the Higgs mass diverge quadratically, as was shown in Eqs. (1.39). The correction has the form

$$m_h^2 = \delta m_h^2 \sim \frac{\alpha_t}{4\pi} \Lambda^2 \quad (1.75)$$

A 125-GeV mass would imply $\Lambda \sim 1$ TeV. To solve the little hierarchy problem, we need $\Lambda \gtrsim O(10)$ TeV while keeping m_h around ~ 100 GeV. How can we achieve this? Suppose that we can arrange the prefactor in front of Λ^2 to be not $(\alpha_t/4\pi)$ but $(\alpha_t/4\pi)^2$; that is, if the leading cutoff sensitivity appears not at one-loop but at two-loop order, then the Higgs mass would be

$$m_h^2 \sim \left(\frac{\alpha_t}{4\pi}\right)^2 \Lambda^2 \quad (1.76)$$

and we may obtain $\Lambda \sim 10$ TeV keeping $m_h \sim 100$ GeV. One should remember that this is not a real solution. The problem is just postponed temporarily. It will reappear as we extend the energy beyond the 10-TeV scale. For the moment, however, we

will be content with the temporary solution. The real solution, commonly referred to as the *UV completion*, remains to be solved. The essence of the “little Higgs” is to achieve this extra prefactor ($\alpha_r/4\pi$), that is, to eliminate one-loop correction [61].

A solution to this problem has been proposed [62] by incorporating an enlarged symmetry and embedding two parallel global symmetry breaking in such a way as to compensate the two competing corrections with each other so that only a logarithmic divergence appears. This is referred to as *collective symmetry breaking*. To reproduce the SM Higgs, one has to start with a larger group G . The collective symmetry breaking assumes that G breaks down to a subgroup H which contains $SU(2) \times U(1)$ in the SM. The Higgs appears as an NGB of the broken symmetry. But under normal circumstances, the gauge interaction will induce quadratically divergent contributions to the Higgs mass as in the SM. To avoid this, one assumes that G contains a subgroup consisting of two copies of $SU(2) \times U(1)$: $G \supset H_1 \times H_2 = [SU(2)_1 \times U(1)_1] \times [SU(2)_2 \times U(1)_2]$. The trick is to arrange this in such a way that each H_i commutes with a different subgroup $Y \supset [SU(2) \times U(1)]_{\text{SM}}$. When X , a subgroup of G ($G \supset X \supset Y$), is gauged, the Higgs mass is still protected by the global symmetry of H_1 and H_2 .

The group structure of the little Higgs is illustrated in Figure 1.13.

Many models have been proposed. As the group structure of realistic models is rather complicated, we discuss a toy model [28] to understand the mechanism of the collective symmetry breaking, which is the essence of the little Higgs model.

Collective Symmetry Breakdown For simplicity, we omit the $U(1)$ part of the SM and start with a global group $G = SU(3)_L \times SU(3)_R$ breaking to $H = SU(2)_L \times SU(2)_R$. We consider two sets of scalar fields in the fundamental representation that transform independently according to

$$\Sigma_L \rightarrow \Sigma'_L = e^{-i\alpha_L} \Sigma_L, \quad \Sigma_R \rightarrow \Sigma'_R = e^{-i\alpha_R} \Sigma_R \quad (1.77)$$

The primary reason that we need two sets of scalar fields is to compensate the two competing corrections with each other. Another reason is that, by gauging a subgroup of the symmetry, one set of the NGB fields is eaten by the gauge particles and disappear. An example can be seen in Eq. (1.73). There, if the broken

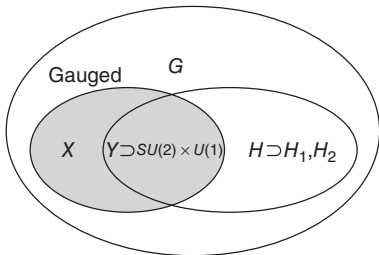


Figure 1.13 Group structure of the little Higgs model. A global group G spontaneously breaks down to H at a scale $f = \Lambda/4\pi$. The origin of the symmetry breaking is irrelevant below the scale Λ . H must

contain $SU(2) \times U(1)$ as a subgroup so that, when a part of G , labeled X , is weakly gauged, the unbroken electroweak group $Y = SU(2) \times U(1)$ comes out [61].

symmetry is the gauged $SU(2)$, the NGBs would be absorbed by the gauge bosons of $SU(2)$ and totally disappear. By preparing two sets, at least half of them survive to become the Higgs we want. For compensation, the two scalar fields need to communicate with each other. Therefore, the symmetry to be gauged has to include both contributions equally. It can be achieved by reformulating the two symmetry groups into diagonal groups.

$$\begin{aligned} SU(3)_L \times SU(3)_R \\ \rightarrow SU(3)_V \times SU(3)_A = SU(3)_{L+R} \times SU(3)_{L-R} \end{aligned} \quad (1.78)$$

The two fields (Σ_L and Σ_R) will transform as $\mathbf{3}$ under $SU(3)_V$ and as $\mathbf{3}$ and $\bar{\mathbf{3}}$ under $SU(3)_A$. By gauging $SU(3)_V$, both of them couple to the same gauge fields and thus are able to communicate with each other.

The twofold $SU(3)$ with $8 + 8 = 16$ generators end up with $3 + 3$ unbroken generators corresponding to the two $SU(2)$ groups. This means that $(8 - 3) \times 2 = 10$ generators are broken, thereby yielding 10 massless NGBs. After gauging $SU(3)_V$, five of the NGBs are eaten up, giving mass to five gauge bosons but the other NGBs remain massless at this stage. The onset of the gauge interaction does not break the symmetry at the tree level, but breaks it when higher order terms, that is, radiative corrections, are taken into account. We will come back to this subject shortly.

Denoting the VEV of the symmetry breaking as f , the low-energy (i.e., $E \ll f$) dynamics can be described by two sets of scalars denoted as Σ_1 and Σ_2 :

$$\begin{aligned} \Sigma_1(x) &= e^{i\theta_1 f} \begin{bmatrix} 0 \\ 0 \\ f + \rho_1(x) \end{bmatrix} = e^{i\theta_E/f} e^{i\Phi(x)/f} \begin{bmatrix} 0 \\ 0 \\ f + \rho_1(x) \end{bmatrix} \\ \Sigma_2(x) &= e^{i\theta_2 f} \begin{bmatrix} 0 \\ 0 \\ f + \rho_2(x) \end{bmatrix} = e^{i\theta_E/f} e^{-i\Phi(x)/f} \begin{bmatrix} 0 \\ 0 \\ f + \rho_2(x) \end{bmatrix} \end{aligned} \quad (1.79)$$

$$\begin{aligned} \Phi(x) &= \sum_{a=1}^5 h_a(x) t_{3+a} = \frac{1}{\sqrt{2}} \begin{bmatrix} 0 & 0 & h^+ \\ 0 & 0 & h^0 \\ h^- & h^{0*} & 0 \end{bmatrix} + \frac{\eta}{2\sqrt{3}} \begin{bmatrix} 1 & 0 & 0 \\ 0 & 1 & 0 \\ 0 & 0 & -2 \end{bmatrix} \\ h^\pm &= \frac{h_1 \mp ih_2}{\sqrt{2}}, \quad h^0 = \frac{h_3 - ih_4}{\sqrt{2}}, \quad \eta = h_5 \end{aligned} \quad (1.80)$$

$\rho_{1,2}$ are real scalar fields that have condensed to acquire the VEV f . They have heavy mass $\sim f$ and are integrated out in the effective field theory.¹⁵⁾ The above choice of VEV leaves the $SU(2)_L \times SU(2)_R$ part of the symmetry unbroken. The phase fields θ_E are eaten up by the gauge fields, or are gauged away in mathematical terms. That is, by suitable gauge transformation they are removed from the NGB sector to become third components of the gauge bosons. $t_a = \lambda_a/2$, $a = 4 - 8$ are $SU(3)$ broken generators and λ_a are the Gell-Mann matrices. One sees that the complex scalar $H = \begin{pmatrix} h^+ \\ h^0 \end{pmatrix}$ forms an $SU(2)$ doublet and the real η a singlet. That the field

15) This is a fancy expression to say that at low energies contributions of $\rho_{1,2}$ are negligible.

Φ satisfies the $SU(2)$ symmetry can be seen as follows: Denoting U_2 as $SU(3)$ transformation matrix which conserves its $SU(2)$ part

$$U_2 = \begin{bmatrix} \hat{U}_2 & 0 \\ 0 & 1 \end{bmatrix} \quad (1.81)$$

it is easy to show that Φ obeys the usual $SU(2)$ transformation law $\Phi' = \hat{U}_2 \Phi \hat{U}_2^\dagger$.

$$\begin{aligned} \Sigma \rightarrow \Sigma' &= U_2 \Sigma = U_2 e^{i\theta_\varepsilon/f} e^{i\Phi/f} U_2^\dagger U_2 \begin{bmatrix} 0 \\ 0 \\ f + \rho_1 \end{bmatrix} = e^{i\theta'_\varepsilon/f} e^{i\Phi'/f} \begin{bmatrix} 0 \\ 0 \\ f + \rho_1 \end{bmatrix} \\ \Phi' &= U_2 \Phi U_2^\dagger = U_2 \frac{1}{\sqrt{2}} \begin{bmatrix} 0 & 0 & h^+ \\ 0 & 0 & h^0 \\ h^- & h^{0*} & 0 \end{bmatrix} U_2^\dagger + U_2 \frac{\eta}{2\sqrt{3}} \begin{bmatrix} 1 & 0 & 0 \\ 0 & 1 & 0 \\ 0 & 0 & -2 \end{bmatrix} U_2^\dagger \\ &= \frac{1}{\sqrt{2}} \begin{bmatrix} 0 & \hat{U}_2 H \\ H^\dagger \hat{U}_2^\dagger & 0 \end{bmatrix} + \frac{\eta}{2\sqrt{3}} \begin{bmatrix} 1 & 0 & 0 \\ 0 & 1 & 0 \\ 0 & 0 & -2 \end{bmatrix} \end{aligned} \quad (1.82)$$

The symmetry breaking has happened at the scale f , which is higher than the EW symmetry breaking scale, that is, $f \gg v_{\text{EW}} = 246 \text{ GeV}$. $H(x)$ will become the Higgs field of the SM, but at this stage they are simply massless NGBs.

The effective Lagrangian is expressed in terms of field derivatives because of the shift symmetry, as shown in Eq. (1.73) and (1.74). Note that the shift symmetry not only prohibits the mass term but also forbids the gauge couplings as well as the Yukawa couplings. The identity $\Sigma^\dagger \Sigma = f^2$ constrains the number of independent operators that can be written at each order in the derivative expansion of the Lagrangian. The leading term contains only one term, $\mathcal{L}_2 = \partial_\mu \Sigma^\dagger \partial^\mu \Sigma$, and contains no mass term. By gauging the $SU(3)_V$ part, the dominant Lagrangian is converted to

$$\begin{aligned} \mathcal{L} &= (D_\mu \Sigma_1)^\dagger (D^\mu \Sigma_1) + (D_\mu \Sigma_2)^\dagger (D^\mu \Sigma_2) \\ D_\mu &= \partial_\mu + ig A_\mu^a t_a \quad (a = 1 \sim 8) \\ \text{where } \Sigma_1 &= e^{i\Phi/f} \begin{bmatrix} 0 \\ 0 \\ f \end{bmatrix}, \quad \Sigma_2 = e^{-i\Phi/f} \begin{bmatrix} 0 \\ 0 \\ f \end{bmatrix} \end{aligned} \quad (1.83)$$

The Lagrangian Eq. (1.83) describes an effective theory valid only at low energies and is unrenormalizable. The cutoff energy Λ and the symmetry breaking VEV f is related by $\Lambda \simeq 4\pi f$. A simple way to see this is to look at the analogous situation in the SM where the radiative correction of the Higgs loop to the mass is given by $\Delta m_h^2 \simeq \lambda^2 (\Lambda/4\pi)^2$ [see Eq. (1.39c)]. A requirement that it should not exceed the tree level Higgs mass $m_h^2 = 2\lambda v^2$ gives $\Lambda \simeq 4\pi v$.

The Gauge Interaction The gauge interaction induces radiative corrections to the mass and connects the two fields by diagrams described in Figure 1.14. Out of eight gauge bosons, three (the $SU(2)$ part) remain massless, which we call W_L , and

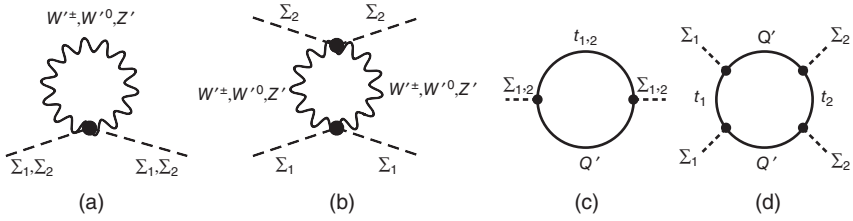


Figure 1.14 Radiative corrections to the Higgs potential. Gauge corrections (a) yield quadratic cutoff dependence which does not contribute to the Higgs potential because W , Z and W' , Z' contributions cancel each other, (b) yields log-divergent contribution to the Higgs mass. The Yukawa

corrections (c) yields quadratic cutoff dependence which does not contribute to the Higgs potential because t and T contributions cancel each other, (d) yields the log-divergent contribution. $Q' = (t_L, b_L, T_L)$, $t_{1,2} = (T_R \pm it_R)/\sqrt{2}$.

will become the SM gauge bosons later. The remaining five will acquire masses of order f and constitute a $SU(2)$ complex doublet (W'^+ , W'^0) and a singlet Z' (to be mixed with yet to enter $U(1)$ group).

After cutting off the loop integral at Λ , Figure 1.14 produces a Higgs potential in the Lagrangian

$$-\frac{g^2}{16\pi^2}\Lambda^2(\Sigma_1^\dagger\Sigma_1 + \Sigma_2^\dagger\Sigma_2) \quad (1.84)$$

As $\Sigma_i^\dagger\Sigma_i = f^2 = \text{constant}$, it does not produce anything. The shift symmetry of Φ is at work here. From the symmetry point of view, the field H contained in Φ is rotated away because of the $SU(2)$ invariant form of $\Sigma^\dagger\Sigma$ which guarantees vanishing mass of the NGBs. For the mass generation of Φ , the Lagrangian has to have some symmetry-breaking term. Let us look at Figure 1.14b. This produces a term

$$-\frac{g^4}{16\pi^2} \ln\left(\frac{\Lambda^2}{f^2}\right) \left|\Sigma_1^\dagger\Sigma_2\right|^2 \quad (1.85)$$

The quadratic divergence terms are canceled between the massless and the massive gauge bosons. So if $\Sigma_1^\dagger\Sigma_2$ constrains the quadratic $H^\dagger H$ terms, we have fulfilled what we had aimed. Expanding Σ_1 and Σ_2 in terms of Φ , we have

$$\begin{aligned} \Sigma_1 &= e^{i\Phi/f} \begin{bmatrix} 0 \\ 0 \\ f \end{bmatrix} = \left(1 + i\frac{\Phi}{f} - \frac{\Phi^2}{2f^2} + \dots\right) \begin{bmatrix} 0 \\ 0 \\ f \end{bmatrix} = \begin{bmatrix} ih^+/\sqrt{2} \\ ih^0/\sqrt{2} \\ f\left(1 - \frac{H^\dagger H}{4f^2}\right) \end{bmatrix} + \dots \\ \Sigma_2 &= \begin{bmatrix} -ih^+/\sqrt{2} \\ -ih^0/\sqrt{2} \\ f\left(1 - \frac{H^\dagger H}{4f^2}\right) \end{bmatrix} + \dots \end{aligned} \quad (1.86)$$

where the ellipses \dots contain higher order terms as well as η -dependent terms. Then

$$\begin{aligned}\Sigma_1^\dagger \Sigma_2 &= -\frac{1}{2}(H^\dagger H) + f^2 \left(1 - \frac{H^\dagger H}{4f^2}\right)^2 + \dots = f^2 - (H^\dagger H) + \frac{(H^\dagger H)^2}{16f^2} + \dots \\ \therefore \left|\Sigma_1^\dagger \Sigma_2\right|^2 &= -2f^2(H^\dagger H) + \frac{9}{8}(H^\dagger H)^2 + \dots\end{aligned}\tag{1.87}$$

Thus we have produced a bilinear term as well as a quartic term of the scalar potential that is necessary to reproduce the SM. Notice that the sign of the bilinear term is negative and that of the quartic term is positive as is required for the symmetry breaking and the stability of the potential.¹⁶⁾ After the symmetry breaking, the Higgs mass is given by

$$m_h^2 \simeq \frac{g^4}{16\pi^2} f^2 \ln\left(\frac{\Lambda^2}{f^2}\right) \sim O\left[\left(\frac{f}{4\pi}\right)^2\right]\tag{1.88}$$

where the last equality follows from $\Lambda \simeq 4\pi f$, $g^4 \ln(4\pi)^2 \simeq 1$. As $m_h \sim O(100)$ GeV, we have $f \simeq 4\pi m_h \sim 1$ TeV, $\Lambda \simeq 4\pi f \sim 10$ TeV. Thus the scale Λ of new physics has been pushed off to the safety zone as required by the EW precision data keeping the Higgs mass light.

Yukawa Interaction So far, we have discussed only the gauge field correction to the mass. Now we want to investigate the contribution of the Yukawa, that is, the top quark, interaction. As the original symmetry is $SU(3)$, the fermion in the fundamental representation contains a new fermion field, which we denote as T . Let us consider a left-handed $SU(3)$ triplet $Q_L^T = (t_L, b_L, T_L)$ and singlets t_R, b_R, T_R . The top quark Yukawa interaction in the SM gives a dangerously large quadratically divergent contribution to the Higgs mass term as we saw in Eq. (1.39a)]. To achieve the same collective symmetry breakdown as the gauge interaction, we expect that contributions of the top quark and the new quark T will compensate each other. Contributions of the other quarks are negligible. Their mass is much smaller.

16) Both coefficients of the quadratic and quartic terms are suppressed simultaneously in this simple model. However, a realistic model should have suppression on the bilinear term but not on the quartic term. If both terms are suppressed, it is not possible to

simultaneously obtain the correct W boson and phenomenologically acceptable Higgs mass. In the more realistic model, this is achieved by enlarging G to $[SU(4)]^4$, which breaks to $H = [SU(3)]^4$, but this is a complication we will not enter into.

When the symmetry breaks down to $SU(2)$ by the scalar VEVs, the part $Q_L^T = (t_L, b_L)$ inside Q'_L transforms as a doublet under the $SU(2)$. With the following $SU(3)$ -invariant Yukawa interaction Lagrangian

$$\begin{aligned} \mathcal{L}_{\text{Yukawa}} &= \frac{h_t}{\sqrt{2}} \left[t_1^c \Sigma_1^\dagger Q'_L + t_2^c \Sigma_2^\dagger Q'_L \right] \\ h_t &= h_t^{(1)} = h_t^{(2)}, \quad t_{1,2} = \frac{1}{\sqrt{2}}(T_R \pm it_R) \end{aligned} \quad (1.89)$$

where $h_t^{(i)}$ s are the top Yukawa coupling constants, one can show [61] that the diagrams shown in Figure 1.14c, d exactly yield contributions as given in Eq. (1.84) and Eq. (1.85) in which g is replaced with h_t . Hence, Figure 1.14c gives a quadratically divergent integral for each t and T but cancel each other. Figure 1.14d gives only a logarithmically divergent integral. Thus the collective symmetry breakdown cancellation mechanism is also at work for the Yukawa interaction.

To construct a viable model, we have to extend the symmetry to include $U(1)$ and formulate the whole group structure in such a way as to satisfy phenomenological constraints such as the absence of FCNC. Several models have been proposed.

The most popular model is the littlest Higgs model [63], which is also the most economical in group structure. Its choice of the group is $G = SU(5)$, which breaks to $H = SO(5)$. The subgroup of $SU(5)$ that is gauged is $[SU(2) \times U(1)]_1 \times [SU(2) \times U(1)]_2$, which breaks to $SU(2)_D \times U(1)_Y$. Out of the 14 (=24-10) NGBs generated as a result of $G \rightarrow H$ breakdown, 4 are absorbed by the massive A_H, Z_H, W_H^\pm corresponding to the broken $SU(2) \times U(1)$ generators. The other 10 scalars arrange themselves to form a complex $SU(2)$ doublet H with the right quantum number of the SM Higgs plus a complex $SU(2)$ triplet.

Others include the simplest model [64], the minimal moose [65], etc. For more details, one may refer to reviews [28, 58].

After the formulation of the models, construction of a mathematically consistent and closed framework (i.e., UV completion) remains to be solved.

Finally, notice that in the supersymmetric model, cancellation of the divergence was done between particles with different spins. In the little Higgs model, it is done between particles with the same spin.

Experimental signals for the little Higgs are the existence of heavy W'^\pm, Z' and the new fermion T . It is a common feature of many beyond-the-SM models and will be discussed in Section 3.4.2.

1.7

Production and Detection of Higgs

Although discovery of the Higgs was at the core of the past effort in going beyond the SM, one should not forget that the most important aim is to understand the Higgs mechanism and not just the discovery of the Higgs particle *per se*. In elucidating the Higgs mechanism, we should consider strategies to cover

a broader range of dynamic reactions that are related to the Higgs associated interactions. The Higgs was discovered at LHC. But it is expected that the detailed dynamical structure could only be clarified by an electron collider, that is, the International Linear Collider (ILC).¹⁷⁾ Therefore it is important to understand the methodology of detecting the Higgs at the e^-e^+ collider as well as at the hadron collider. We should be aware of the advantage and disadvantage of the hadron collider compared to the electron collider. In view of this, we first review past LEP experiments for the Higgs search before discussing the detection method at the hadron collider.

1.7.1

Higgsstrahlung $e^-e^+ \rightarrow hZ$

At LEP, the following two production mechanisms were effective (see Figure 1.15)

- At $\sqrt{s} = m_Z$: $e^-e^+ \rightarrow Z \rightarrow hZ^* \rightarrow h\bar{l}l$ (Z^* is virtual). (1.90)
- At $\sqrt{s} > m_Z$: $e^-e^+ \rightarrow Z^* \rightarrow hZ$ (Higgsstrahlung). (1.91)

As $m_h > m_Z$, the process (1.90) is no longer relevant for the future consideration. Therefore, we only consider the Higgsstrahlung. At LEP II ($\sqrt{s} = 200$ GeV), the method to use the Higgsstrahlung [Figure 1.15a] was viable. The selection of events was made by looking at $Z \rightarrow \bar{l}l, q\bar{q}$, requiring the invariant mass of the lepton or quark pair to coincide with m_Z . Identification of $Z \rightarrow \nu\bar{\nu}, h \rightarrow q\bar{q}$ was also possible by requiring “1 jet + missing energy.” This is possible because the total energy of the Zh system is known and the Higgs mass can be reconstructed from the observables. The Higgs was not discovered at LEP, and the obtained upper limit was 114 GeV at 95% CL.

1.7.2

W Boson Fusion

When the Higgs mass goes beyond 100 GeV, the vector boson fusion process ($e^-e^+ \rightarrow e^-e^+V^*V^* \rightarrow e^-e^+h, V = W, Z$) becomes the dominant process in the e^-e^+ collider (see Figure 1.15b, c). Although the gluon fusion is the dominant process at LHC as far as Higgs production is concerned, the W boson fusion will again take over for sufficiently large s . The WW reaction has a unique feature that the gluon fusion does not have. Longitudinal components of W are the would-be-Goldstone bosons of the Higgs, that is, it is a direct result of the spontaneous symmetry breaking. In fact, there exists an equivalence theorem that, at sufficiently high

17) The ILC is considered as the next major project in particle physics. It is an electron-positron collider using straight linacs stretching up to 20 km in length. The energy has

not been decided yet but is envisaged to start from ~ 500 GeV eventually going over 1 TeV. It could be set lower to optimize for the Higgs study.

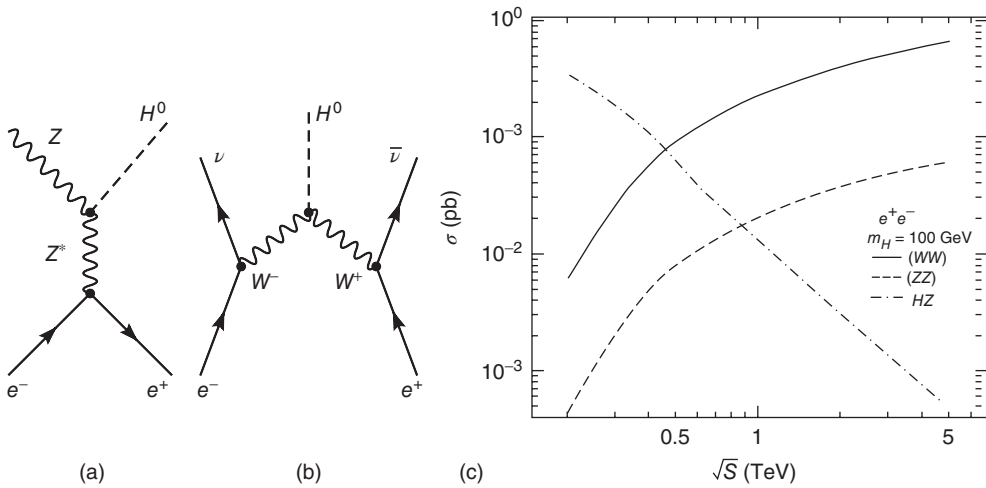


Figure 1.15 Higgs production mechanisms and their total cross section. (a) Higgsstrahlung: $e^-e^+ \rightarrow Z^* \rightarrow Zh$. Valid for $m_Z < \sqrt{s} \lesssim 300$ GeV and 60 GeV $< m_h < 100$ GeV. (b) W boson fusion: $e^-e^+ \rightarrow W^-W^+ \rightarrow h$. Valid for $\sqrt{s} > 300$ GeV and $m_h > 100$ GeV.

(c) Total cross section for the Higgs production via vector boson fusion in e^-e^+ annihilation as a function of \sqrt{s} when $m_h = 100$ GeV. The total cross section for the process $e^-e^+ \rightarrow hZ$ is also shown for comparison. (Reproduced with permission of [66].)

energy ($s \gg m_W^2$), $W_L W_L$, $W_L Z_L$ scattering are equivalent to the scatterings between the would-be-Goldstone bosons (h^0 , h^\pm) [67]. In this regard, the WW reactions are inherently suited to elucidate the dynamics of the Higgs mechanism.

In order to understand the WW reaction mechanism, including the Higgs production at the hadron collider, we first study the idea of boson fusion and the equivalent W approximation in the electron collider. In the hadron collider, the main QCD processes are not the quark–quark interactions but the gluon–gluon reaction. It is related partly to the large coupling of the gluon but also has its origin in the vanishing mass of the gluon. In the EW production of the Higgs at the hadron collider, the total energy is large enough so that $\hat{s} \gg m_W^2$, where \hat{s} is the total energy of the elementary process of interest (i.e., partons). At such high energies, even the gauge bosons can be regarded as nearly massless and we expect the boson–boson interactions to play an important role just like the gluon–gluon interactions in QCD. In this respect, we can make use of the tools we acquired in quantum electrodynamics (QED). The following discussion is provided to prepare the WW scattering as one of main tools for probing the dynamics of the Higgs sector after the discovery of the Higgs particle.

Equivalent W Approximation As for the boson fusion cross section, an exact formula in the tree approximation exists [66, 68], but the effective W approximation,

which is easier to understand intuitively, gives a good approximation (error $< 20\%$) and we will use it hereafter. This is an application of the Weiszäker–William approximation (see Section 17.6.3 of [1]). It replaces an electromagnetic e – A (A represents an atom) process by the equivalent γ^* – A process where the almost-real photon flux is provided by the electron. Replacing the photon with W and the electromagnetic coupling by the EW coupling, one gets the equivalent W approximation. In other words, the equivalent W approximation is valid at the high energy where the relevant total energy \hat{s} is sufficiently large compared to the W mass. Then the Bremsstrahlung formula in QED can be used, which almost restricts the W emission in the forward region ($\theta \approx 0$). One may recall that a similar consideration was adopted in formulating the DGLAP (Dokshitzer–Gribov–Lipatov–Altarelli–Parisi) evolution equation in QCD to compute the parton flux. Here, the electron is replaced by the quark, and the virtual photon by the gluon.

In phenomenological expressions, the W mass is retained in the propagator, which provides a natural cutoff below $p_T < m_W$. In this approximation, we consider the incoming e^-/e^+ beam as a supplier of the gauge boson flux. Once we get an equivalent flux function, it can be treated like the parton distribution functions in QCD, and the WW , ZZ , ZW scattering formula can be constructed using factorization formulas as used in hadron–hadron collisions.

Let us start from the W bremsstrahlung by an electron. Extension to that by a quark is straightforward. Assume that the electron with energy-momentum p_1 and the positron with p_2 are the suppliers of the colliding W s with momenta $x_1 p_1$ and $x_2 p_2$ of the parents $e^- e^+$ and that its flux is given by $F(x_1)$ and $F(x_2)$. The cross section for the Higgs production $\sigma(e^- e^+ \rightarrow e^- e^+ h; s)$ can be expressed in terms of the vector boson fusion process cross section $\sigma(VV \rightarrow h; \hat{s})$:

$$\sigma(e^- e^+ \rightarrow e^- e^+ h; s) = \int dx_1 dx_2 F(x_1) F(x_2) \hat{\sigma}(VV \rightarrow h; \hat{s}) \quad (1.92)$$

$$\hat{s} = x_1 x_2 s$$

For $m_h^2 \gg m_W^2$ and $\tau = m_h^2/s$

$$\begin{aligned} \hat{\sigma}(VV \rightarrow h) &= \frac{16\pi^2 m_h}{\hat{s}} \Gamma(h \rightarrow VV) \delta(\hat{s} - m_h^2) \\ &= \frac{16\pi^2 m_h}{\hat{s}^2} \Gamma(h \rightarrow VV) \tau \delta(x_1 x_2 - \tau) \end{aligned} \quad (1.93)$$

Substituting Eq. (1.93) into Eq. (1.92), we obtain

$$\sigma(e^- e^+ \rightarrow e^- e^+ h) = \frac{16\pi^2 m_h}{\hat{s}^2} \Gamma(h \rightarrow VV) \tau \frac{dL}{d\tau} \quad (1.94)$$

where

$$\frac{dL}{d\tau} = \int_{\tau}^1 \frac{dx}{x} F(x) F\left(\frac{\tau}{x}\right) \quad (1.95)$$

$dL/d\tau$ is the luminosity of the WW flux that the $e^- e^+$ beam provides. Substituting the expression for the decay rate [Eqs. (1.19)] into the above expression, we

obtain

$$\sigma(e^-e^+ \rightarrow e^-e^+h) = \frac{\pi^2\alpha}{\sin^2\theta_W m_W^2} \tau \frac{dL}{d\tau} \quad (1.96)$$

Kinematics of the W flux in $e \rightarrow e + W$ prepared by its parent particle is the same as that of the gluon flux in QCD with replacements of the coupling constant and symmetry factors. Thus the flux of W prepared by the electron can be obtained using the same formula as used to derive the splitting functions in QCD.

$$F(x) = \frac{g^2}{8\pi^2} P_{BC \leftarrow A}(x) \quad (1.97)$$

$$P_{BC \leftarrow A}(x) = \frac{x(1-x)}{2} \frac{\overline{\sum} |V(A \rightarrow BC)|^2}{p_T^2 + (1-x)m_W^2} \quad 18)$$

where g is the coupling constant of W/Z with the electron. Despite the inherent zero-mass approximation for the W bremsstrahlung, the mass term in the denominator was retained to provide a natural cutoff at small p_T . Substituting actual expressions of the ($e \rightarrow e + W$) Lagrangian, one gets

$$g^2 \overline{\sum} |V(A \rightarrow BC)|^2 = \overline{\sum} |\bar{u}(p_C) \not{\epsilon}(g_V - g_A \gamma^5) u(p_A)|^2 \quad (1.99)$$

Here, g_V and g_A are the vector and the axial-vector coupling strength and are different for $V = W$ or $V = Z$. Using

$$W : \quad g_V = g_A = \frac{g_W}{2\sqrt{2}}$$

$$Z : \quad g_V = \frac{g_Z}{2} (I_3 - 2Q \sin^2 \theta_W), \quad g_A = \frac{g_Z}{2} I_3 \quad (1.100)$$

$$g_W = \frac{e}{\sin \theta_W}, \quad g_Z = \frac{e}{\sin \theta_W \cos \theta_W}$$

18) This is a general formula [69] to calculate the splitting function in QCD when a parton "a" splits into partons "b" and "c," the former having fractional momentum $p_b = xp_a$ and the latter $p_c = (1-x)p_a$, except that in QCD the mass is set to zero.

$$F_{bc \leftarrow a} = \frac{\alpha_s}{2\pi} \left[\frac{x(1-x)}{2} \frac{\overline{\sum} |V(a \rightarrow bc)|^2}{p_T^2} \right] \quad (1.98)$$

See Appendix K of [2].

$$d\sigma(a + d \rightarrow c + X)$$

$$\simeq F_{bc \leftarrow a}(x) dx \frac{d\phi}{2\pi} d \ln p_T^2 d\sigma(b + d \rightarrow X)$$

one calculates the flux for $\hat{s} \gg m_W^2$ to obtain [70, 71]

$$F_T(x) = \frac{(g_V^2 + g_A^2)}{8\pi^2} \frac{1 + (1-x)^2}{x} \ln \left(\frac{\hat{s}}{m_W^2} \right) \quad (1.101a)$$

$$F_L(x) = \frac{(g_V^2 + g_A^2)}{4\pi^2} \frac{(1-x)}{x} \quad (1.101b)$$

The luminosity function $F_T(x)$ for the transversely polarized W is identical to the Weiszäcker–Williams formula (see Eq. (17.89) of [1]) for the photon flux given by the electrons if one replaces $(g_V^2 + g_A^2)/(4\pi) \rightarrow \alpha$. Substituting Eqs. (1.101) in Eq. (1.95), one gets the VV luminosity for the transversely and longitudinally polarized gauge bosons [72].

$$\left. \frac{dL}{d\tau} \right|_{ee/V_T V_T} = \left[\frac{g_V^2 + g_A^2}{8\pi^2} \right]^2 \left[\ln \frac{\hat{s}}{m_W^2} \right]^2 \frac{1}{\tau} \left[(2 + \tau)^2 \ln \frac{1}{\tau} - 2(1 - \tau)(3 + \tau) \right] \quad (1.102a)$$

$$\left. \frac{dL}{d\tau} \right|_{ee/V_L V_L} = \left[\frac{g_V^2 + g_A^2}{4\pi^2} \right]^2 \frac{1}{\tau} \left[(1 + \tau) \ln \frac{1}{\tau} - 2(1 - \tau) \right] \quad (1.102b)$$

The Higgs production cross section becomes [66, 68, 72]

$$\begin{aligned} \sigma(e^-e^+ \rightarrow e^-e^+h) &= \left(\frac{\alpha}{\sin^2 \theta_W} \right)^3 \frac{1}{16m_h^3} \left[\frac{m_h^3}{m_W^2} \left\{ (1 + \tau) \ln \frac{1}{\tau} - 2(1 - \tau) \right\} \right. \\ &\quad \left. + \frac{m_W^2}{2m_h} \left(\ln \frac{\hat{s}}{m_W^2} \right)^2 \left\{ (2 + \tau)^2 \ln \frac{1}{\tau} - 2(1 - \tau)(3 + \tau) \right\} \right] \end{aligned} \quad (1.103)$$

The first line is the contribution of the longitudinal W , and the second line is that of the transverse W 's.

1.7.3

Productions at the Hadron Collider

The main mechanism of the Higgs production at the LHC is gluon fusion, and the submechanism is vector boson fusion. Their Feynman diagrams are shown in Figure 1.16a,c. Two other reactions that can be used to identify the Higgs are $t\bar{t}h$ -associated production (Figure 1.16d) and Higgsstrahlung by the quarks (Figure 1.16e).

Gluon Fusion The production cross section of the Higgs by gluon fusion is given by [73, 74]

$$\begin{aligned} \sigma(pp \rightarrow pph) &= 2 \times \frac{1}{4} \times \frac{1}{64} \times \frac{16\pi^2}{m_h^3} \Gamma(h \rightarrow gg) \tau \frac{dL}{d\tau} \\ \frac{dL}{d\tau} &= \int dx_1 dx_2 \delta(x_1 x_2 - \tau) g(x_1) g(x_2) \end{aligned} \quad (1.104)$$

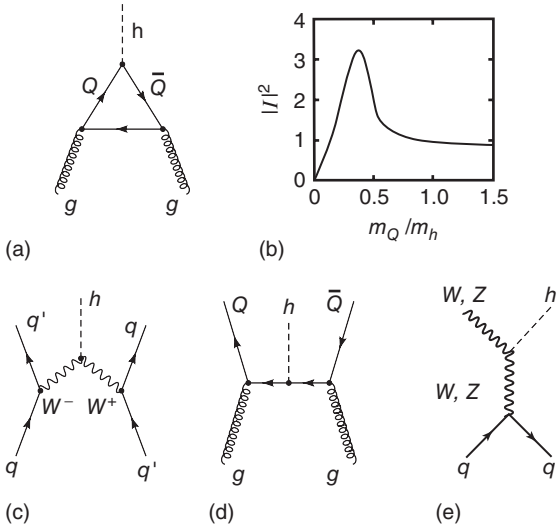


Figure 1.16 Feynman diagrams for the Higgs production. (a) Gluon fusion. (b) Shape of the loop integral of the gluon fusion diagram. (c) Boson fusion. (d) $t\bar{t}h$ -associated production. (e) QCD + EW production

where $g(x)$ is the gluon distribution function in the proton. The extra factors in front of $\Gamma(h \rightarrow gg)$ relative to Eq. (1.94) (1/4, 1/64) are due to spin and color degrees of freedom of the gluon, and the factor 2 is due to the Bose–Einstein statistics of the two gluons. The decay width of $h \rightarrow gg$

$$\Gamma(h \rightarrow gg) = \frac{\sqrt{2}G_F[\alpha_s(m_h)]^2}{8\pi^3} \frac{m_h^3}{9} |I|^2 \quad (1.105)$$

can be derived from an effective Lagrangian

$$\mathcal{L}_{hgg} = -(\sqrt{2}G_F)^{\frac{1}{2}} \frac{\alpha_s(m_h)}{12\pi} IG_{\mu\nu} G^{\mu\nu} h \quad (1.106)$$

where $G_{\mu\nu}$ is the gluon field strength. Here, the quantity I originates from fermion loops and is given by

$$I = \sum_j I_j = N_c \sum_j \int_0^1 dx \int_0^{1-x} dy \frac{1 - 4x\gamma}{1 - x\gamma \left(\frac{m_h^2}{m_j^2} \right) - i\epsilon} \quad (1.107)$$

The spectral shape of the loop integral for the gluon fusion $|I|^2$ is plotted in Figure 1.16b. Its value is dominated by the heaviest quark, that is, the top. $|I|^2$ takes a maximum value 3.2 for $\lambda_Q = m_Q/m_h \simeq 0.4$ and $|I|^2 \simeq 1$ for $\lambda_Q \gtrsim 1$. For $\lambda_Q \ll 1$, $|I|^2 \sim (\lambda_Q \log \lambda_Q)^4$. That is, $\sigma(gg \rightarrow h)$ decreases like $\lambda_Q^4 \sim 1/m_h^4$. The total production cross section of the Higgs in the hadron collider which incorporates NNLO in QCD [75] is given in Figure 1.17. The largest cross section comes from $\sigma(gg \rightarrow h)$, which is the top line. The broad bump in the cross section reflects the shape of the loop integral.

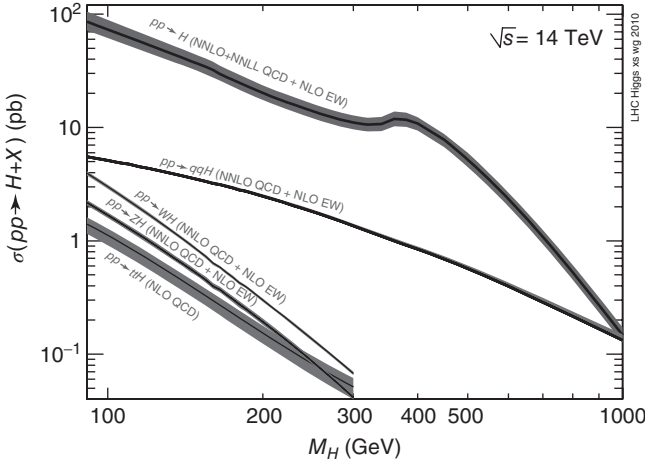


Figure 1.17 SM Higgs boson production cross sections for pp collisions at 14 TeV. The top line is due to the gluon fusion, and the line $pp \rightarrow qqH$ denotes the W boson fusion. Other channels are also indicated. (Reproduced with permission of [8, 76, 77].)

Luminosity of W Boson Fusion The W flux provided by a quark is identical to that by an electron except for replacement of $e - W$ coupling with $q - W$ coupling. The quark flux, in turn, is provided by the proton in a hadron collider. Therefore, the Higgs production through WW fusion in the hadron collider can be obtained from that of the electron collider by convoluting with parton distribution functions. Or, equivalently, the W luminosity in the pp reaction is given by convoluting that of e^-e^+ collision with the parton distribution functions $f_i(x)$ [70, 71].

$$\left. \frac{dL}{d\tau} \right|_{pp/VV} = \sum_{ij} \int dx_1 dx_2 f_i(x_1) f_j(x_2) \times \left[\int d\xi d\eta F(\xi) F(\eta) \delta(x_1 \xi x_2 \eta - \tau) \right] \quad (1.108)$$

Putting $x_1 x_2 = \tau'$, the content of $[\dots]$ is expressed as

$$\frac{1}{\tau'} \int \frac{dx}{x} F(x) F\left(\frac{\tau'}{x}\right) = \frac{1}{\tau'} \left. \frac{dL}{d\xi} \right|_{\xi=\tau/\tau'} \equiv \frac{1}{\tau'} \left. \frac{dL}{d\xi} \right|_{qq/VV} \quad (1.109)$$

The WW luminosity in the pp collision becomes

$$\left. \frac{dL}{d\xi} \right|_{pp/VV} = \sum_{ij} \int_{\tau}^1 \frac{d\tau'}{\tau'} \int_{\tau'}^1 \frac{dx}{x} f_i(x) f_j\left(\frac{\tau'}{x}\right) \left. \frac{dL}{d\xi} \right|_{qq/VV} \quad (1.110)$$

Then the cross section is given by

$$\sigma(pp \rightarrow VV \rightarrow h; s) = \int_{\tau}^1 d\tau \left. \frac{dL}{d\tau} \right|_{pp/VV} \hat{\sigma}(VV \rightarrow h; \tau s) \quad (1.111)$$

where the variables in $\hat{\sigma}(VV \rightarrow h)$, $dL/d\xi|_{qq/VV}$ are to be replaced from those of the electron collision to those of the quark collision. The reduction rate of the W boson

fusion cross section as a function of m_H is much slower than that of the gluon fusion cross section. So, it will eventually dominate over the gluon fusion, but at the LHC the dominant contribution still comes from the gluon fusion. Detailed calculations at NLO (next-to-leading order) in QCD have been obtained by [78, 79]. Figure 1.17 gives the most recent plot on the cross sections including other channels [8, 77]. The main contributions to the Higgs production cross sections come from gluon or W fusions, but some other modes are also useful for obtaining better S/N (signal-to-noise ratio) by identifying the accompanying particles.

1.7.4

Signals at LHC

We already know that the Higgs was discovered with mass in the neighborhood of 125 GeV. Nevertheless, we discuss possible signals of Higgs production and decays in the various mass regions because the discovery alone is not our final goal. We want to study the dynamics of the Higgs, and it is useful to consider how it would change if the Higgs mass was different. Study of competing processes is also important.

In the e^-e^+ reaction, the competing processes possess physical meanings of their own right. All the open channels have branching ratios of the same order (see Figure 1.18a), and are useful in elucidating one aspect of the physics or another.

Considering channels other than that of specific interest as noises, the S/N in the e^-e^+ reaction is at most of the order of 100. Therefore, if enough number of events are obtained, it is relatively easy to identify the produced Higgs by looking at its decay products such as $h \rightarrow jj$ (2 jets), $\bar{l}l$ ($l = e, \mu, \tau$). In the two-body production $e^-e^+ \rightarrow Zh$, the invariant mass of the Higgs can be obtained by simply identifying the Z.

But in hadron productions, backgrounds due to QCD processes are large and S/N for the Higgs production is minuscule, as can be seen from Figure 1.18b. To illustrate the difficulty of the event selection in the hadron collider, we show a typical event display at the LHC in Figure 1.19. There are ~ 25 vertices per beam crossing. The bunch crosses every 25 ns, totaling up to 600 million collisions per second. A signal in such a proliferation of events is literally a needle in a haystack.

One has to choose the decay channels carefully to identify the parent Higgs, depending on its mass.

At LHC, for a luminosity of $L = 10^{34}/\text{cm}^{-2}/\text{s}^{-1}$.¹⁹⁾ one can obtain in a year (assume 1 year = 10^7 s) $\int L = 10^{41}/\text{cm}^{-2} = 100 \text{ fb}^{-1}$. For the process having a total cross section 1 pb one can obtain 10^5 Higgs particles. Let us investigate whether this number is sufficient to discover the Higgs. As the decay branching ratio changes as a function of the mass (see Figure 1.2) and backgrounds for each channel are different, an optimum detection method has to be adopted depending on the mass value. As the experimental lower limit had already reached a value $m_h = 114$ GeV before the LHC, we consider cases for a mass larger than this value. The following

19) The improved design luminosity is up to $5 \times 10^{34}/\text{s}^{-1}/\text{cm}^{-2}$. So this is a modest number.

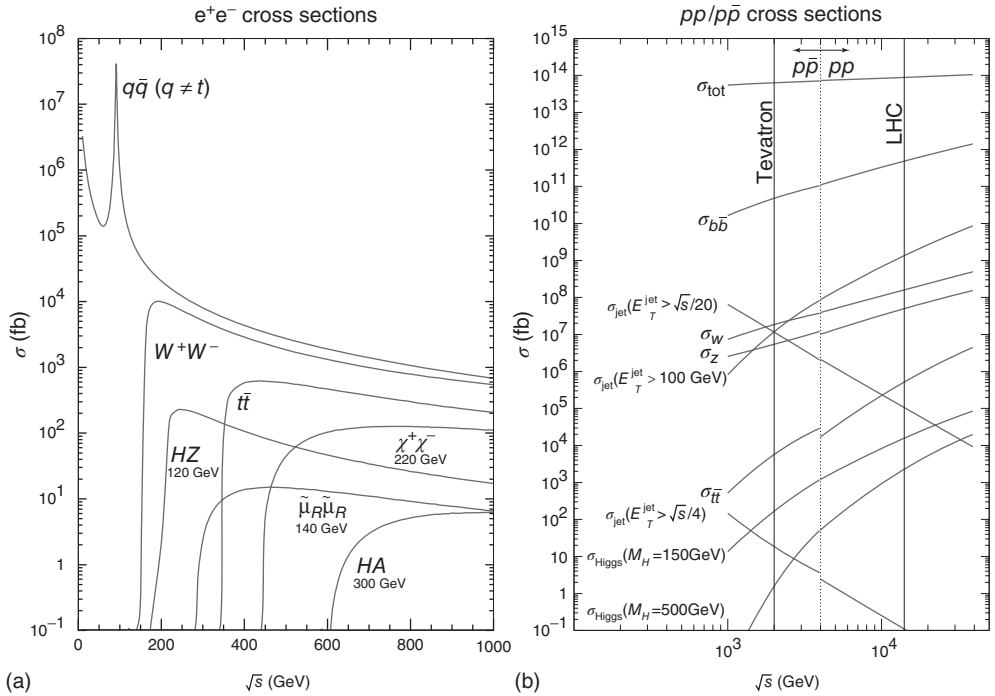


Figure 1.18 Production cross sections for several representative processes at e^+e^- colliders (a) and hadron colliders (b), as a function of the machine center-of-mass energy. (Reproduced with permission of [80].)

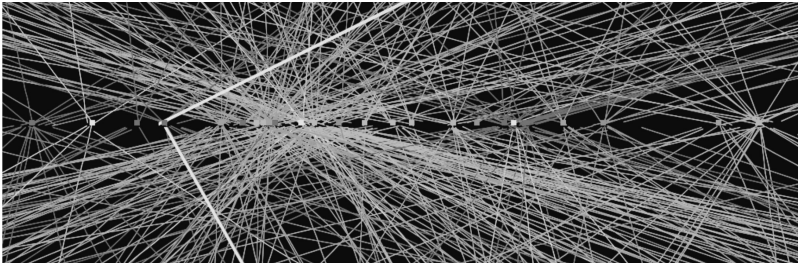


Figure 1.19 Event display for a trigger per beam crossing in the ATLAS detector with 25 reconstructed vertices. This event happened to include a $Z \rightarrow \mu\mu$ event. The display with track p_T threshold of 0.4 GeV and all tracks are required to have at least three pixels and six SCT (SemiConductor Tracker) hits. (Reproduced with permission of [81, 82].)

list is only an example. Although we have listed some useful modes in discovering the Higgs for particular mass range, most of the modes can be used eventually at any mass range as the intensity goes up and backgrounds are better understood. Comparison of observed data with them will provide important information on the properties of the Higgs.

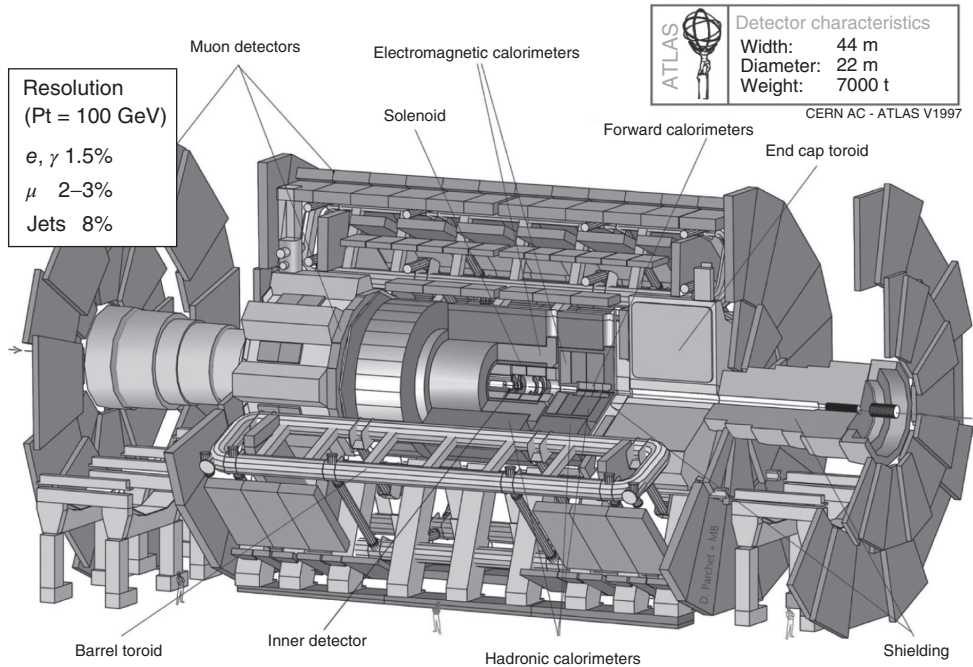


Figure 1.20 ATLAS (A Toroidal LHC Apparatus) is a general-purpose detector with balanced performance including hadronic events. Its magnet is an air-cored one with inner (outer) radius 5 (10)m and length 26 m, and produces a field strength of 0.8 T (2 T at the center). The electromagnetic calorimeter is a liquid argon detector of

accordion shape [see Figure 12.35 of [1]]. The overall size is $20\phi \times 44$ m, and weighs 6000 tons. Resolutions are good but not particularly good for all measurements. (Reproduced with permission of [83].) (Please find a color version of this figure on the color plates.)

Two large general-purpose detectors, ATLAS and CMS were constructed and are in operation (see Figure 1.20, 1.21). The CMS has a better resolution for gamma/lepton signals but is less versatile for hadron detection. Components of the general purpose collider detectors and their functions were explained in Section 12.6 of [1]. Two special purpose detectors, LHCb for the B-physics and Alice for the heavy ion collisions were also constructed.

1.7.5

Higgs Detection Methods

(1) $110 \text{ GeV} < m_h < 130 \text{ GeV}$ $h \rightarrow \gamma\gamma$: For the mass $m_h < 2m_W$, $h \rightarrow b\bar{b}$ is the main decay mode. However, the QCD background is overwhelming and their separation is difficult. Looking at Figure 1.2, there exists a usable mode $h \rightarrow \gamma\gamma$ with a branching ratio of $\sim 10^{-3}$. That is, in the inclusive decay mode

$$p + p \rightarrow h + X, \quad h \rightarrow \gamma + \gamma \quad (1.112)$$

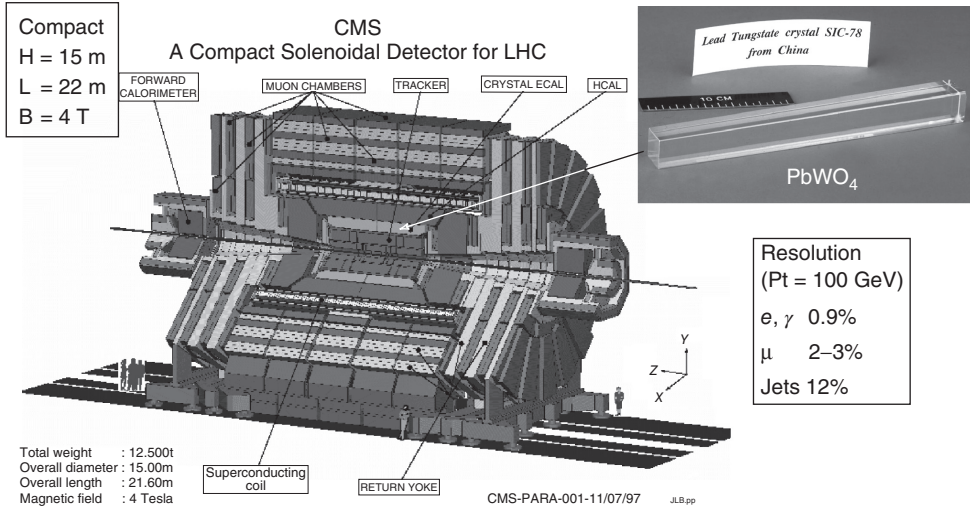


Figure 1.21 CMS (compact muon solenoid) is a detector at LHC. The length is about one-half of that of the ATLAS detector but its weight (= 12.5 kton) is twice that of ATLAS. It uses PbWO_4 (lead glass) for the electromagnetic calorimeter and realizes a resolution of 0.9% (1.5%) at $P_T = 100$ GeV. The

magnetic field strength is 4 T as compared to 2 T of ATLAS. It excels in $e/\mu/\gamma$ physics and is general purpose, but is less versatile for hadron detection. (Reproduced with permission of [84].) (Please find a color version of this figure on the color plates.)

one catches two γ 's and identifies their parent Higgs by reconstructing the 2γ invariant mass. However, catching 2γ alone may suffer from large backgrounds due to 2γ production by QCD and misidentification of QCD jets. One needs a γ detector (electromagnetic calorimeter) with high energy resolution [3, 85]. This is a clean channel but needs high luminosity.

$t\bar{t}h$ ($h \rightarrow b\bar{b}$): Another method is to use associated production accompanied with W or $t\bar{t}$ in $q\bar{q} \rightarrow WhX$, $t\bar{t}hX$ and identify isolated leptons from W or $t\bar{t}$. With this method, one can obtain cleaner signals, but the problem is whether one can get enough statistics [86–88]. The experimental groups ATLAS and CMS are capable of discovering the Higgs in this decay mode within the mass range 80 – 130 GeV [89, 90].

(2) $120 \text{ GeV} < m_h < 180 \text{ GeV}$ $h \rightarrow ZZ^* \rightarrow 4l$: This is a golden mode in the search for the Higgs. Although the mass value is too low to decay to two real Z's, production of four leptons through virtual Z intermediate states is possible. This channel is promising for the range $120 < m_h < 180$ GeV except for the narrow region around 170 GeV (see Figure 1.2).

$h \rightarrow \tau\bar{\tau}$ ($m_h < 140$ GeV): One looks for $\mu^\pm +$ missing energy + X [91]. The Higgs mass cannot be reconstructed in this channel, but the signal can be observed as an excess of events above backgrounds which come mainly from WWX and $t\bar{t} \rightarrow WWb\bar{b} \rightarrow l\bar{l}\nu\bar{\nu}$.

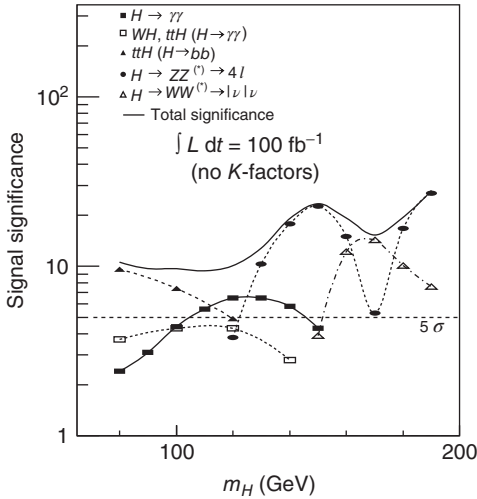


Figure 1.22 ATLAS sensitivity for the discovery of a Standard Model Higgs boson for integrated luminosities of 100 fb^{-1} data in the $m_H < 200$ -GeV range. The dotted line is the 5σ significance

level. The figure was taken from design studies for the detector construction of the ATLAS. The actual results are much better. (Reproduced with permission of [94, 95].)

$h \rightarrow W^- W^+ \rightarrow \bar{l} l \bar{\nu} \nu$ ($m_h \sim 170 \text{ GeV}$) [92, 93]: For the Higgs mass nearing $2m_Z$, the signal significance in the $h \rightarrow ZZ^* \rightarrow 4l$ channel is reduced because of the suppression of the ZZ^* branching ratio as the WW decay mode opens up. For $m_h = 170 \text{ GeV}$, $h \rightarrow WW^* \rightarrow \bar{l} l \bar{\nu} \nu$ branching ratio is approximately 100 times larger than that of the $h \rightarrow ZZ^* \rightarrow 4l$ channel. However, because of the presence of the neutrino, it is not possible to reconstruct the true Higgs mass. Instead, an excess of events may be observed. The transverse mass

$$m_T = \sqrt{2p_T^l E_T^{\text{miss}}(1 - \cos \Delta\phi)} \quad (1.113)$$

is expected to fall in the mass window $m_h - 30 \text{ GeV} < m_T < m_h$. Here, p_T^l , E_T^{miss} , and $\Delta\phi$ are momentum of the lepton pair, the missing transverse energy, and the azimuthal angle in the transverse plane, respectively.

We summarize the Higgs discovery sensitivity of the ATLAS detector below $m_h = 200 \text{ GeV}$ in Figure 1.22 for integrated luminosity of 100 fb^{-1} [20].

(3) $180 \text{ GeV} < m_h < 800 \text{ GeV}$ $h \rightarrow ZZ \rightarrow 4l$: If the Higgs mass is larger than $2m_Z$, the main decay modes are WW and ZZ pairs. Hadronic decay modes are difficult to separate completely from QCD backgrounds. The cleanest signal can be obtained

20) Notice that the Higgs was discovered with an integrated luminosity of 5 fb^{-1} at 7 TeV.

from purely leptonic decay modes

$$\begin{aligned}
 p + p &\rightarrow h + X \\
 h &\rightarrow Z + Z \rightarrow e^- e^+ (\mu^- \mu^+) + e^- e^+ (\mu^- \mu^+)
 \end{aligned}
 \tag{1.114}$$

This decay mode is referred to as the *gold-plated channel* [96–99]. As the branching ratio is 1.1×10^{-3} , the signal size is not large. But by requiring the invariant mass of the two pairs of leptons $m_{\ell\bar{\ell}} = m_Z$, one can reduce a large amount of the background. The main components of the background include ZZ continuous spectrum production and Zbb , $Zt\bar{t}$.

(4) $700 \text{ GeV} < m_h < 1000 \text{ GeV}$ $h \rightarrow ZZ \rightarrow \ell\bar{\ell}\nu\bar{\nu}$:

The discovery capability using the $h \rightarrow ZZ \rightarrow 4\ell$ decay mode goes down as the mass goes up and hits the limit at around 800 GeV. This is mainly due to the reduction of the counting rate but also because the width becomes large ($\Gamma_h > 250 \text{ GeV}$). The resonance is no longer a sharp peak but a slow bump and is hard to identify. There is also a theoretical question as to whether such a wide resonance can be considered as a particle.

To extend the mass range, one needs to use other channels that include neutrinos in the final state. For the large-mass Higgs, if the hermeticity of the detector is good (i.e., if a condition that the missing energy vector can be well defined for large rapidity holds), one may be able to reconstruct the missing energy. The Higgs signal in this case appears as the Jacobian peak in the transverse momentum,²¹⁾ a fact that is utilized in identifying the W boson at the Tevatron. Because of the facts that one cannot reconstruct the invariant mass and the width becomes large, one may not be able to expect a sharp peak in the event distributions. The signal appears as an excess over the background, and therefore understanding the background is very important for the detection of the Higgs using the missing energy.

In summary, the LHC was designed to discover the SM Higgs having mass $110 \text{ GeV} < m_H < 1 \text{ TeV}$. It covers the entire mass range that is theoretically allowed.

1.7.6

Discovery of Higgs

Both ATLAS and CMS groups announced the discovery of Higgs-like particles at the mass value $m_h \simeq 125 \text{ GeV}$ in the summer of 2012. We present the signals in the decay channels $h \rightarrow \gamma\gamma$ in Figure 1.23 and $h \rightarrow 4\ell$ in Figure 1.24.

The Higgs-like boson was produced with approximately the right values for production cross sections as well as for branch decay modes that are expected for the Higgs in the SM.

21) A peak at the edge of a spectrum that appears by a sharp cutoff of kinematic variables (in this case p_T).

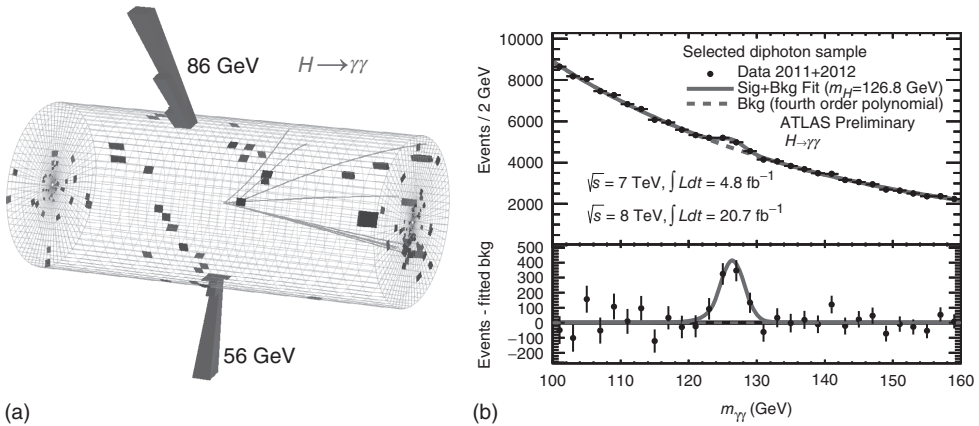


Figure 1.23 (a) CMS event display for the Higgs in the $h \rightarrow 2\gamma$ mode. (Reproduced with permission of [100,101].) (b) Invariant mass distribution of diphoton candidates for the combined $\sqrt{s} = 7$ TeV and $\sqrt{s} = 8$ TeV data samples obtained by ATLAS. The result of a fit to the sum of a

signal component fixed to $m_H = 126.8$ GeV and a background component described by a fourth-order Bernstein polynomial are superimposed. The bottom inset displays the residuals of the data with respect to the fitted background component. (Reproduced with permission of [102].)

1.7.7

SM Higgs?

The question arises whether the discovered Higgs-like particle is really the SM Higgs or something similar to it in other models.

Spin Parity of the Higgs The spin parity of the Higgs-like particle is converging to 0^+ , although statistics are poor at this stage (summer, 2013). The CMS group analyzed the spin parity of the Higgs using a kinematic discriminant which includes the description of the interference of identical leptons in the $4e$ and 4μ final states. The discriminant adopts the matrix element likelihood approach (MELA) which uses

$$D_{J^P} = \frac{\mathcal{P}_{\text{SM}}}{\mathcal{P}_{\text{SM}} + \mathcal{P}_{J^P}} = \left[1 + \frac{\mathcal{P}_{J^P}(m_{Z_1}, m_{Z_2}, \vec{\Omega} | m_{4l})}{\mathcal{P}_{\text{SM}}(m_{Z_1}, m_{Z_2}, \vec{\Omega} | m_{4l})} \right]^{-1} \quad (1.115)$$

as a discriminant between the different spin-parity hypotheses. Here, \mathcal{P}_{SM} is the probability distribution for the SM Higgs boson hypothesis, and \mathcal{P}_{J^P} is the probability for an alternative model. Figure 1.25a shows the distributions of D_{J^P} . Distributions in data (points with error bars) and expectations for background and signal are shown for the alternative hypothesis between 0^+ and 0^- . Figure 1.25b shows a distribution of $q = -2 \ln(\mathcal{L}_{J^P} / \mathcal{L}_{\text{SM}})$ for the 0^+ and 0^- hypothesis. The arrow indicates the observed value.

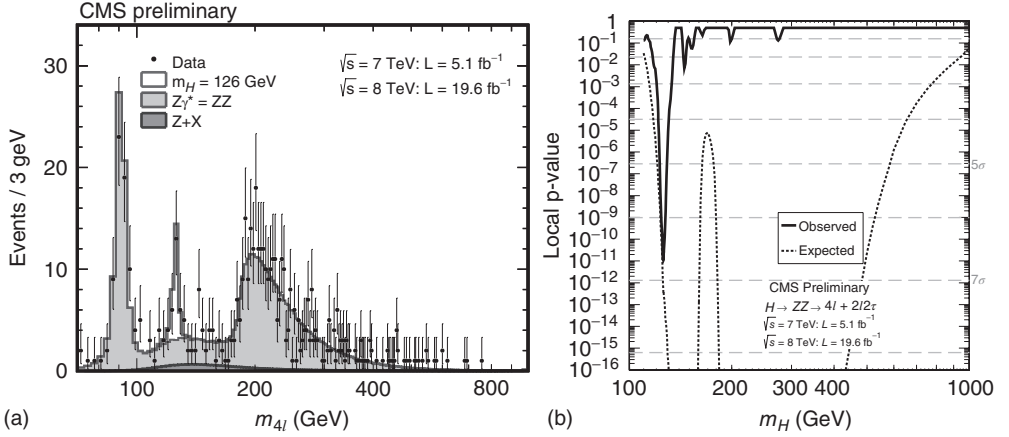


Figure 1.24 (a) CMS data. Distribution of the four-lepton reconstructed mass in the full mass range for the sum of the $4e$, 4μ , and $2e2\mu$ channels. Points represent the data, shaded histograms represent the background, and the unshaded histogram represents the signal expectation. The expected distributions are presented as stacked histograms. The measurements are presented

for the sum of the data collected at $\sqrt{s} = 7$ TeV and $\sqrt{s} = 8$ TeV. No event is observed for $m_{4l} > 800$ GeV. (b) Significance of the local excess (right) with respect to the SM background expectation as a function of the Higgs boson mass in the full interpretation mass range 110–1000 GeV. (Reproduced with permission of [103].)

Table 1.5 shows a summary result of the spin-parity analysis.

The analysis (Table 1.5) favors 0^+ as the J^P assignment of the Higgs-like particle.

Coupling Strength The best way to determine whether the observed particle is the SM Higgs is to measure its coupling strength. In the SM, the coupling strength and the mass are directly related by $m_f = \gamma_f v / \sqrt{2}$ for the fermion and $m_V = g_V v / 2$ for the vector boson where $v = 246$ GeV is the VEV of the Higgs. The probability to observe a particular Higgs production and decay mode, say, $gg \rightarrow h \rightarrow ff$, is proportional to

$$\sigma \cdot BR(gg \rightarrow h \rightarrow ff) = \frac{\sigma_{gg} \cdot \Gamma_{ff}}{\Gamma_H} = \sigma_{SM} \cdot BR_{SM} \cdot \left(\frac{\kappa_g^2 \kappa_{ff}^2}{\kappa_H^2} \right) \quad (1.116)$$

where Γ_H , Γ_{ff} , etc. are total decay width of the Higgs and partial decay width for $h \rightarrow ff$. The variables $\kappa_{ff}^2 = \Gamma_{ff} / \Gamma_{ff,SM}$ are the ratios of the coupling strength to those of the Standard Model. When the mass of the Higgs is fixed to the observed value $m_H = 125$ GeV, all the decay widths can be calculated. Therefore, the ratio $\mu \equiv (\sigma \cdot B)_{ob} / (\sigma \cdot B)_{SM}$ is a measure of how good the SM assumption is.

As an example, we show a test of the gluon-fusion production of the Higgs versus vector boson fusion production. Figure 1.26a shows the measured μ s for various channels keeping only the two production couplings ($(gg \rightarrow H) + (gg \rightarrow t\bar{t}H)$ and the vector fusion process ($V^* \rightarrow VH$)) free. As one is looking at the same decay channels, all the uncertainties in the decay processes cancel each other and one

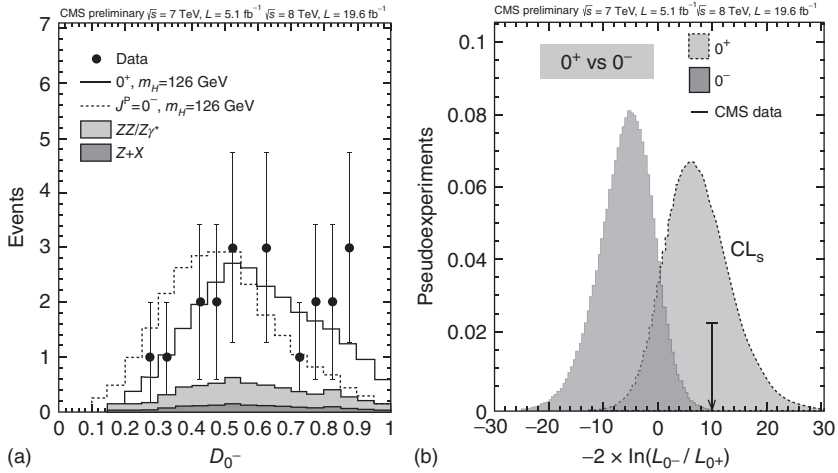


Figure 1.25 Spin analysis using $h \rightarrow ZZ^* \rightarrow 4l$ data, showing the kinematic discriminant built to describe the kinematics of production and decay of different J^P states of a “Higgs. The left figure shows D_{0^-} distribution with a requirement $D_{bkg} = \mathcal{P}_{sig}/(\mathcal{P}_{sig} + \mathcal{P}_{bkg}) > 0.5$. The arrow in the right figure indicates the observed value. (Reproduced with permission of [103, 104].)

Table 1.5 List of models used in analysis of spin-parity hypotheses corresponding to the pure states of the type noted.(Reproduced with permission of [103, 104].)

J^P	Production	Comment	Expect $\mu = 1$	Observed 0^+	Observed J^P	CLs
0^-	$gg \rightarrow X$	Pseudoscalar	2.6σ (2.8σ)	0.5σ	3.3σ	0.16%
0^+_h	$gg \rightarrow X$	Higher dim operators	1.7σ (1.8σ)	0.0σ	1.7σ	8.1%
$2^+_{m_{gg}}$	$gg \rightarrow X$	Minimal couplings	1.8σ (1.9σ)	0.8σ	2.7σ	1.5%
$2^+_{m_{qq}}$	$gg \rightarrow X$	Minimal couplings	1.7σ (1.9σ)	1.8σ	4.0σ	<0.1%
1^-	$gg \rightarrow X$	Exotic vector	2.8σ (3.1σ)	1.4σ	> 4.0σ	<0.1%
1^+	$gg \rightarrow X$	Exotic Pseudovector	2.3σ (2.6σ)	1.7σ	> 4.0σ	<0.1%

The expected separation is quoted for two scenarios when the signal strength for each hypothesis is predetermined from the fit to data (0^P model) and when events are generated with SM expectation for the signal yield ($\mu = 1$). The observed separation quotes consistency of the observation with the 0^+ model or the J^P model, and corresponds to the scenario when the signal strength is predetermined from the fit to data. The last column quotes the confidence level criterion for the J^P model.

can see the difference of the production mechanism. No deviations from the SM is observed.

Because of multichannel productions in the hadron collider, the accuracy of the coupling constants that can be obtained at LHC has some limitations. We show how they can be improved if an electron–positron linear collider is used [Figure 1.26b] [106]. The discovered Higgs-like particle indeed behaves like the SM Higgs.

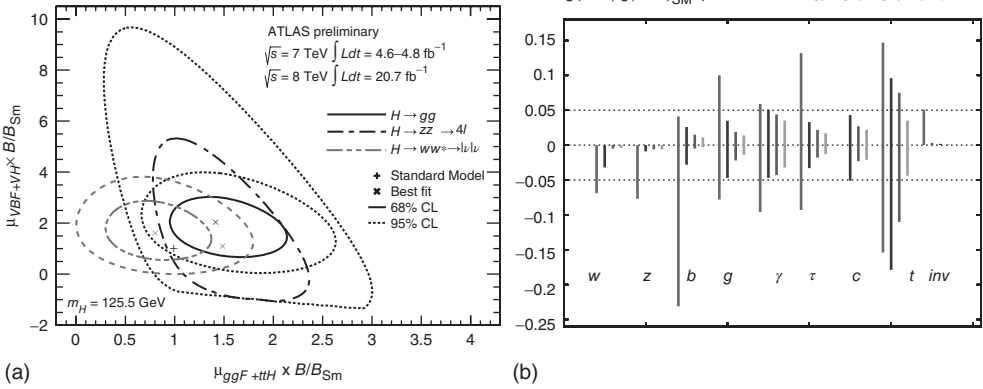


Figure 1.26 (a) Comparison of gluon–gluon fusion and vector boson fusion for the production of the Higgs and subsequent decays to various channels. $\mu = 1$ corresponds to the Standard Model. (Reproduced with permission of [105].) (b) Comparison of the capabilities of LHC and ILC for model-independent measurements of the Higgs boson couplings. The plot shows (from left

to right in each set of error bars) 1σ confidence intervals for LHC at 14 TeV with 300 fb^{-1} , for ILC at 250 GeV and 250 fb^{-1} ('ILC1'), for the full ILC program up to 500 GeV with 500 fb^{-1} ('ILC2'), and for a program with 1000 fb^{-1} for an upgraded ILC at 1 TeV ('ILCTeV') (Reproduced with permission of [106].)

1.7.8

MSSM Higgs and Future Prospect

Neutral Higgs Next, we investigate whether the Higgs fits to the SUSY. The detection method for the neutral Higgs (H^0 , h^0 , A^0) in the MSSM at the electron collider is almost identical to that of the SM Higgs with increased degrees of freedom given by the existence of A^0 . In addition to channels $e^-e^+ \rightarrow h^0 Z^*$, $h^0 A^0 \rightarrow \tau\tau b\bar{b}$, a four-jet final state was also available. Figure 1.27a shows the excluded region on the m_{h^0} - $\tan\beta$ plane obtained at the LEP collider. The discovered Higgs is also compatible with its interpretation as the light Higgs h^0 in SUSY for small ($\ll 1$) and large ($\gg 1$) $\tan\beta$.

Prospects at LHC The discovery method of MSSM Higgses at the hadron collider is similar to that of the SM Higgs. The difference is that the number of Higgs species has increased and it affects the decay branching ratios. Figure 1.27a shows the excluded region by LEP in the $(m_h - \tan\beta)$ plane. Figure 1.27b shows the ATLAS team's work on their capability of finding one or more of the MSSM Higgs using various methods with an integrated luminosity of 300 fb^{-1} . Although parameters may have been taken a little optimistically, one sees that all the regions are covered. The LHC has the capability of discovering at least one of the neutral members of the Higgs in the MSSM [35, 94, 108].

If the light Higgs is discovered at LHC, one still has to distinguish whether it is the SM Higgs or that of SUSY. To pinpoint the parameter values, it is necessary to

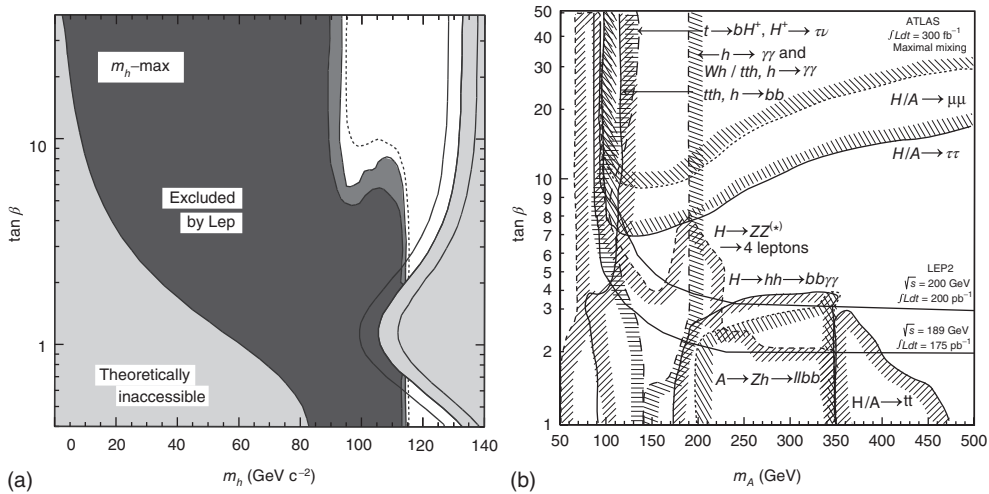


Figure 1.27 (a) MSSM light Higgs exclusion contours by LEP experiments, at 95% CL (light-green/middle-right thin gray region) and 99.7% CL (dark-green/dark gray region). The figure shows the excluded and theoretically inaccessible regions in the $(m_h, \tan \beta)$ projection. The upper edge of the theoretically allowed region is sensitive to the

top quark mass; it is indicated, from left to right, for $m_t = 169.3, 174.3,$ and 179.3 . (Reproduced with permission of [7, 107].) (b) Predicted 5σ discovery contours for MSSM Higgs boson detection in various channels in the $m_A - \tan \beta$ plane. (Reproduced with permission of [35, 94, 108].)

determine the decay branching ratios or to discover directly the charged Higgs or CP-odd A^0 . Figure 1.28a shows the excluded regions by the LHC on the $m_A - \tan \beta$ plane prior to the discovery of the Higgs.

The discovery of the Higgs particles at $m_h = 125$ GeV, if interpreted as the light Higgs of the MSSM, constrains the allowed region. Figure 1.28b shows the allowed band (green band) at the tree level with $m_h = 125 \pm 3$ GeV limit [111]. The dark (blue) areas are the excluded regions by LEP and Tevatron/LHC [109, 110], and the gray area is the allowed region like the one shown in the left figure prior to the discovery of the Higgs particle. Note, however, that the limit is obtained by choosing other parameters governing the higher order corrections such that a maximum value for m_h is obtained (m_h^{\max} benchmark scenario). While the lower limit is fairly stable, the upper limit is strongly dependent on the choice of the parameters. Therefore, at this stage, the green band should be interpreted only as the most favorable parameter region. The gray region above the band is disfavored but by no means prohibited.

Charged Higgs The charged Higgs can be produced at the LEP through the reaction

$$e^- + e^+ \rightarrow H^- + H^+ \quad (1.117)$$

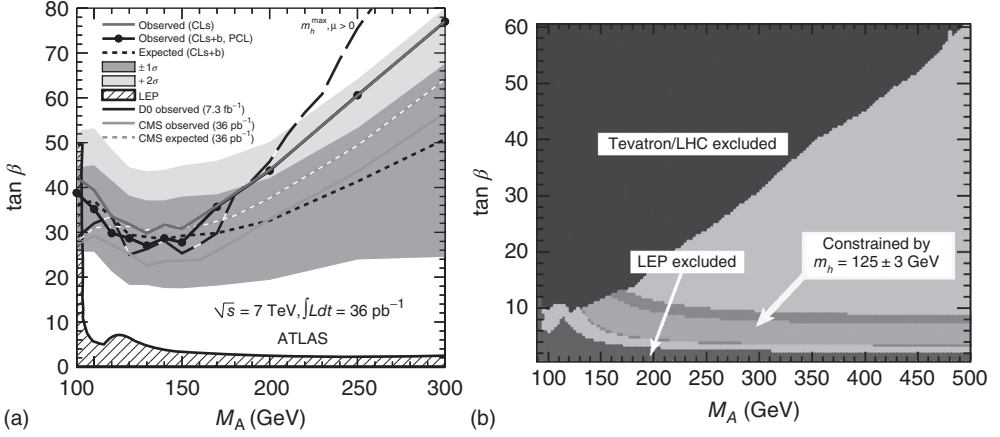


Figure 1.28 (a) Expected and observed exclusion limits in the $m_A - \tan\beta$ plane of the MSSM without the Higgs at 125 GeV. The region above the drawn limit curve is excluded at the 95% CL for the $m_h = \text{max}$ scenario. The dark gray (green) and light gray (yellow) bands correspond to the $\pm 1\sigma$ and $+2\sigma$ error bands, respectively. The exclusion limits from LEP, D0, and CMS are also shown. (Reproduced with permission of [109, 110].) (b) Discovery of the Higgs particle at $m_h = 125$ GeV, if interpreted as the light Higgs of the MSSM constrains the allowed region on the $m_A - \tan\beta$ plane. The green horizontal band shows the region where m_h is compatible with the observed value within errors (125 ± 3 GeV).

The brighter green is for the top mass value $m_t = 173.2$ GeV and the dark green corresponds to $\pm 1\sigma = 0.9$ GeV variation. The parameters governing the higher order corrections are taken such that a maximum value for m_h is obtained (m_h^{max} benchmark scenario). Dark (blue) areas are the excluded regions by LEP and Tevatron/LHC (see (a)). The gray area is the allowed parameter space prior to the latest LHC results. Note: Constraints on the upper edge of the green band is loose. This is still preliminary. If the $m_h = \text{max}$ scenario is modified, the allowed region can be expanded to above significantly. (Reproduced with permission of [111–113].) (Please find a color version of this figure on the color plates.)

The Higgs decays preferentially to heavy particles. At the LEP, the main decay modes are $H^+ H^- \rightarrow \tau^+ \nu \tau^- \nu$ and $(c\bar{s})(\bar{c}s)$. Referring to Eq. (1.51), one can show

$$\frac{BR(H^+ \rightarrow \tau^+ \nu)}{BR(H^+ \rightarrow c\bar{s})} \approx \frac{m_\tau^2 \tan^4 \beta}{3m_c^2} \quad (1.118)$$

As the detection of the H^+ in both leptonic and hadronic decay modes is possible in the electron collider, the lower limit of the m_{H^\pm} independent of the value of $\tan\beta$ was obtained by the LEP2 [114].

$$m_{H^\pm} > 79.3 \text{ GeV} \quad [8] \quad (1.119)$$

At the hadron collider, the charged Higgs boson can be produced in different modes, but for $m_{H^\pm} < m_t - m_b$ it can be produced via the decay $t \rightarrow bH^+$, $H^\pm \rightarrow \tau\nu$. In the top quark decays, the W bosons decay equally to leptons of the three generations, while H^+ may decay predominantly into $\tau\nu$. Hence, an excess of $t\bar{t}$

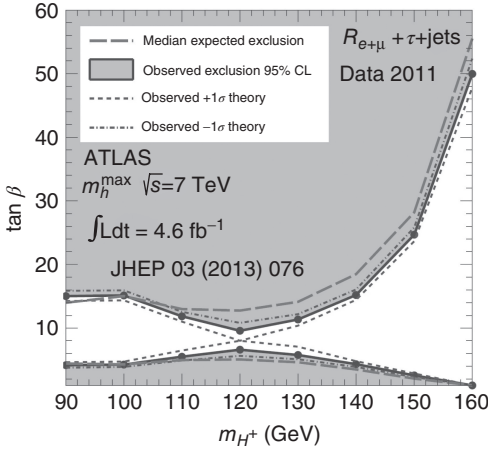


Figure 1.29 Summary of the 95% CL exclusions in the $(m_{H^\pm}, \tan \beta)$ plane obtained by ATLAS [115]. The mass range below 90 GeV was excluded by the Tevatron. [116–118] (Reproduced with permission of [115].)

events with at least one hadronically decaying τ lepton (τ_{had}) in the final state, as compared to the rate for $t\bar{t}$ events with only electrons and/or muons, is a signature for charged Higgs bosons. One can use the ratio R_l to determine

$$R_l = \frac{BR(t\bar{t} \rightarrow b\bar{b} + l\tau_{\text{had}} + N\nu)}{BR(t\bar{t} \rightarrow b\bar{b} + ll' + N\nu)} \quad (1.120)$$

where ll' stands for electrons and muons with $l \neq l'$, and $N\nu$ stands for any number of neutrinos. Figure 1.29 shows the excluded region [115].

The mass region below 90 GeV was excluded by the Tevatron experiments [116–118].

As the mass of the charged Higgs is constrained by the relation Eq. (1.59), the discovery of the neutral Higgs at $m_h = 125$ GeV constrains the minimum mass value of the charged Higgs to $m_{H^\pm} > 152 \sim 161$ GeV [111]. This means that the detection of the charged Higgs in the decay channel of $t \rightarrow b + H^\pm$ is nearly excluded.

1.8

Summary

The discovery of the Higgs filled the last vacancy of the SM particles. But it has posed a new problem. The SM explains the EW data so well that it has pushed the boundaries of new physics beyond the limits predicted by many theoretical considerations. The mass of the detected Higgs is quite consistent with the predictions made by using the radiative corrections of the SM and the precision EW data obtained at LEP and Tevatron. The problem is that the Higgs is too

light. The SM corrections to the Higgs mass diverge quadratically and, in order to reproduce the observed Higgs mass, the cutoff energy scale is constrained to be at most $\sim O(1\text{TeV})$. It contradicts the EW precision data analysis that no new physics should come in below $O(10)\text{TeV}$. This is the little hierarchy problem.

One possible remedy was the SUSY. It was an aspired-for model because of its many desirable features. The mass value 125 GeV is within the range of predictions of SUSY. But it lies almost at the extreme limit of the allowed range. Many options of the SUSY were excluded. More details of the SUSY will be discussed in Chapter 5. The composite Higgs is another possibility. However, the composite models tend to produce a large mass, and the observed mass is at the low-end limit. To understand the dynamics that govern the Higgs, we need more experimental inputs.

